TOPICAL REVIEW

Infrared Properties of QCD from Dyson-Schwinger equations

Christian S. Fischer

GSI, Planckstr. 1, 64291 Darmstadt, Germany

E-mail: christian.fischer@physik.tu-darmstadt.de

Abstract. I review recent results on the infrared properties of QCD from Dyson-Schwinger equations. The topics include infrared exponents of one-particle irreducible Green's functions, the fixed point behaviour of the running coupling at zero momentum, the pattern of dynamical quark mass generation and properties of light mesons.

PACS numbers: 02.30.Rz, 11.10.St, 12.38.Aw, 12.38.Lg, 14.40.Aq, 14.65.Bt, 14.70.Dj

Contents

1. Introduction

Our understanding how observable properties of hadrons emerge from the underlying structure of the strong interaction is still far from complete. Physical phenomena encountered at large momentum transfers are very well described by perturbation theory. *Asymptotic freedom* allows high energy probes to picture hadrons as lumps of weakly interacting quarks and gluons. This picture, however, starts to break down at intermediate momenta and is surely inadequate at energies below a view hundred MeV. At such scales the interaction is strong enough to invalidate perturbation theory and one has to employ completely different methods to deal with what can be called *Strong QCD*.

There are two fundamental low energy properties of QCD: confinement and dynamical chiral symmetry breaking. Both are entirely strong coupling effects in the sense that they cannot be accounted for at any order in perturbation theory. They are presumably related to each other, although the detailed structure of this relation is not yet clear. Both together are responsible for the complexity of the experimental hadron spectrum. The internal structure of hadrons beyond the simple valence quark model is one of the central issues in contemporary low energy hadron physics. Nonperturbative methods such as lattice Monte-Carlo simulations [1, 2], the exact renormalisation group (see [3] and references therein) or the Green's function approach employing Dyson-Schwinger and Bethe-Salpeter equations [4–7] are appropriate tools to explore the details of these structures.

Dyson-Schwinger and Bethe-Salpeter equations (DSEs/BSEs) are the equations of motion of the Green's functions of a field theory. In QCD the study of the nonperturbative behaviour of these functions is interesting for several reasons. Confinement mechanisms like the Kugo-Ojima criterion or the Gribov-Zwanziger scenario are related to the infrared behaviour of the ghost and gluon propagators. Nonperturbative definitions of the running coupling can be given in terms of renormalisation group invariants constructed from two and three point functions. Effects of dynamical chiral symmetry breaking are encoded in the quark propagator and the quark-gluon interaction. Furthermore, properties of bound states and resonances can be determined from the n-point functions of the theory.

The machinery of DSEs and BSEs has been studied extensively in the last years. From a technical point of view these continuum Green's functions methods and lattice Monte-Carlo simulations are complementary to each other. Lattice calculations contain all effects from quantum fluctuations and are therefore the only *ab initio* approach available so far. However, lattice results are limited to a comparably small momentum range and potentially suffer from finite volume effects in the infrared. The implementation of realistic light quark masses still awaits faster CPUs and better algorithms.

Dyson-Schwinger equations, on the other hand, can be solved analytically in the infrared and provide numerical solutions for a large momentum range. All aspects of

chiral symmetry are respected such that the properties and effects of light quarks can be determined systematically with reasonable effort. A technical challenge of DSEs is that they form an infinite tower of equations which are coupled to each other. Thus, in order to obtain a closed system of equations for n-point functions one has to introduce approximations for some m-point functions with $m > n$ (unless one works in certain kinematical limits, see subsection 2.2). These truncations have to be controlled, *e.g.* by comparison to corresponding lattice calculations in the momentum region where lattice results are available. In turn, however, the Dyson-Schwinger approach provides important information in momentum and quark mass regions that are not (yet) accessible on the lattice.

A note on gauge independence is in order here. In general, Green's functions are gauge dependent objects. Certainly, confinement and dynamical mass generation are experimentally observable phenomena and as such must have gauge independent theoretical signatures. Confinement is encoded in the long distance behaviour of the (gauge invariant) Wilson loop and the strength of dynamical chiral symmetry breaking is given by its (gauge invariant) order parameter, the chiral condensate. On the other hand it is very well possible that the detailed mechanism that generates these quantities depends on the gauge. Furthermore possible order parameters separating the confining from the deconfining phase of gauge theories may only be identifiable after gauge fixing. Therefore the approach to study the theoretical structures leading to these phenomena in different gauge fixed formulations of QCD is justified, interesting and well established (see *e.g.* [1] and reference therein).

This review is intended as an overview on selected topics of nonperturbative QCD. I concentrate on some questions of low energy QCD which to my opinion can be answered particularly well in the DSE/BSE approach. Owing to limited space I focus on QCD at zero temperature and zero density and discuss in some detail recent results that have not yet been included in other reviews. Interesting developments within the DSE/BSE approach at finite temperature or density are described in [6, 8–10]. Furthermore I can only give a brief account on results for various meson observables. Reviews on this subject can be found in [5, 7, 11]. Studies of the baryon sector of QCD employing Faddeev equations are still exploratory. Recent results can be found in [12–16].

2. The Yang-Mills sector of QCD

Confinement, *i.e.* the absence of (coloured) quarks and gluons from the observable spectrum is widely believed to be generated in the gauge sector of QCD‡. This phenomenon should be reflected in the infrared properties of the dressed one-particle irreducible Green's functions of Yang-Mills theory. This is one of the reasons why these functions have been studied in the past. Another reason is that elements of Yang-Mills theory, as *e.g.* the dressed gluon propagator, are vital ingredients for a description of

‡ A different view has been advocated by Gribov, for a review of his ideas see [17].

hadrons via Bethe–Salpeter equations [5, 6]§. Older works on this subject are based on the idea of infrared slavery and assume a gluon propagator that is strongly singular at zero momentum. In the past years this picture has changed and recent studies employing Dyson–Schwinger equations [18–23] or lattice Monte-Carlo simulations [24–27] indicate quite the opposite: an infrared finite or even vanishing gluon propagator. Nonperturbative infrared singularities, however, are predicted to occur in the ghost propagator, the vertices and also in most of the other n-point functions of Yang-Mills theory. I explain the logical structure of the arguments leading to this result in subsection 2.2 and discuss some interesting consequences in the remaining parts of this section. In order to appreciate these results it is useful to first recall some aspects of confinement related to Green's functions.

2.1. Aspects of confinement

QCD is the quantum field theory of quarks and gluons. In Euclidean space-time the partition function is given by‖

$$\begin{aligned} Z[J,\eta,\bar{\eta}] \quad &= \int \mathcal{D}[A\bar{\Psi}\Psi] \exp\left\{ - \int d^4x \left(\bar{\Psi}\left(-\not{D} + m\right)\Psi + \frac{1}{4} F^a_{\mu\nu} F^a_{\mu\nu} \right) \right. \\ &\qquad \left. + \int d^4x \left(A^a_\mu J^a_\mu + \bar{\eta}\Psi + \bar{\Psi}\eta \right) \right\} . \end{aligned} \tag{2.1}$$

Quarks are represented by the Dirac fields Ψ and $\bar{\Psi}$. Local gauge symmetry of the quark fields demands the introduction of a vector field A^a_μ, which represents gluons. External sources for these fields are denoted by $\bar{\eta}$, η and J^a_μ. The gluon field strength $F^a_{\mu\nu}$ is given by

$$F^a_{\mu\nu} = \partial_\mu A^a_\nu - \partial_\nu A^a_\mu - g f^{abc} A^b_\mu A^c_\nu \ , \tag{2.2}$$

with the coupling constant g and the structure constants f^{abc} of the gauge group $SU(N_c)$, where N_c is the number of colours. The covariant derivative in the fundamental representation of the gauge group is given by

$$D_\mu = \partial_\mu + igA_\mu \ , \tag{2.3}$$

with $A_\mu = A^a_\mu t^a$ and the t^a are the generators of the gauge group.

Together the quark and gluon content of the action

$$S_{QCD} = \int d^4x \left(\bar{\Psi}\left(-\not{D} + m\right)\Psi + \frac{1}{4} F^a_{\mu\nu} F^a_{\mu\nu} \right) \tag{2.4}$$

ensures that QCD is invariant under local gauge transformations. Hereby it is assumed that the path integral measure $\mathcal{D}[A\bar{\Psi}\Psi]$ is invariant by itself.

The path integral in (2.1) runs over all possible gauge field and Dirac field configurations. This implies multiple counting of physically equivalent configurations,

§ I discuss this in more detail in section 4.

‖ Detailed explanations of the physical content of the QCD partition function is given in many textbooks, see *e.g.* [28, 29]. An introduction into path integral methods in quantum field theories is given *e.g.* in [30].

i.e. configurations that are connected by a gauge transformation. Therefore the integration generates an infinite constant, the volume of the gauge group $\mathcal{G}$, which has to be absorbed in the normalisation. More important, the gauge freedom implies that the quadratic part of the gauge field Lagrangian has zero eigenvalues and therefore cannot be inverted. This prevents the definition of a perturbative gauge field propagator.

To proceed we introduce the notion of a gauge orbit $[A^g]$, which is a set of gauge configurations that is related by a gauge transformation:

$$[A^g] := \left\{ A^g = gAg^\dagger + gdg^\dagger : g(x) \in SU(N_c) \right\}. \tag{2.5}$$

All elements of a particular gauge orbit are physically equivalent. In order to single out one representative configuration from each orbit one has to impose a gauge fixing condition on the generating functional. This is conveniently done by the Faddeev-Popov procedure [31] (see also [32, 33] for pedagogical treatments of the subject). The idea is to insert the identity

$$1 = \Delta[A^g] \int \mathcal{D}g \, \delta[F(A)] \tag{2.6}$$

into the generating functional (2.1). The gauge fixing condition $F(A) = 0$ is supposed to be satisfied for one and only one gauge field configuration per gauge orbit. The 'Faddeev-Popov determinant' $\Delta[A^g]$ accounts for the functional determinant arising from the argument in the delta function. Problems with this gauge fixing procedure are discussed in more detail below.

In linear covariant gauges the Faddeev-Popov determinant $\Delta[A]$ reads explicitly

$$\Delta[A^g] = \mathrm{Det}\left(-\partial_\mu D^{ab}_\mu\right), \tag{2.7}$$

where $D^{ab}_\mu = \partial_\mu \delta^{ab} + g f^{abc} A^c_\mu$ denotes the covariant derivative in the adjoint representation. This determinant can be written as a functional integral over two new Grassmann valued fields c and $\bar{c}$, the so called 'Faddeev-Popov ghosts'. Also the gauge fixing condition $\delta[F(A)]$ can be represented by a Gaussian integral. We therefore finally arrive at the gauge fixed generating functional of QCD,

$$\begin{aligned} Z[J,\sigma,\bar{\sigma},\eta,\bar{\eta}] = \mathcal{N} \int \mathcal{D}[A\bar{\Psi}\Psi c\bar{c}] \exp\Bigg\{ & - S_{QCD}[A,\Psi,\bar{\Psi}] - S_{gf}[A,c,\bar{c}] \\ & + \int d^4x \left(A^a_\mu J^a_\mu + \bar{\eta}\Psi + \bar{\Psi}\eta + \bar{\sigma}c + \bar{c}\sigma \right) \Bigg\}, \end{aligned} \tag{2.8}$$

with the gauge fixing part

$$S_{gf} = \int d^4x \left(\frac{(\partial_\mu A_\mu)^2}{2\zeta} - i\partial_\mu \bar{c} D_\mu c \right) \tag{2.9}$$

of the action. The first term in S_{gf} stems from the gauge fixing condition and introduces a gauge parameter ζ, whereas the second term represents the Faddeev-Popov determinant. The integral over the gauge group has been absorbed in the overall normalisation $\mathcal{N}$. Note also that new sources σ and $\bar{\sigma}$ for the antighost and ghost fields have been introduced. In the discussion below I frequently refer to Landau gauge, which

is defined by the gauge condition $F(A) = \partial_\mu A_\mu = 0$ and gauge parameter $\zeta = 0$. The corresponding gauge fixing condition of Coulomb gauge is $F(A) = \partial_i A_i = 0$, where $i = 1..3$ counts the spatial components of the gauge field.

Although the action $S_{QCD} + S_{gf}$ is fixed wrt. local gauge transformations, there are two gauge symmetries left: The global gauge symmetry and the so called BRST-symmetry, which has been found by Becchi, Rouet, Stora and Tyutin [34, 35]. Since both will play an important role below, it is appropriate to discuss some of their properties.

The global gauge transformations of the gauge field and the quark field are given by

$$A_\mu \to A'_\mu = e^{it^a\Lambda^a} A_\mu e^{-it^a\Lambda^a} \ , \tag{2.10}$$

$$\Psi \ \to \Psi' = e^{it^a\Lambda^a}\Psi \ , \tag{2.11}$$

with space-time independent parameters Λ^a and the generators t^a of the gauge group. Although the global gauge transformation is a symmetry of the Lagrangian it is not immediately clear whether a corresponding well defined charge exists, *i.e.* whether global gauge symmetry is spontaneously broken or not. This issue will be discussed further below.

A BRST-transformation is formally equivalent to a local gauge transformation with the transformation parameters $\Lambda^a(x)$ replaced by the product of a Grassmann number λ and the ghost field, $\Lambda^a(x) \to \lambda c^a(x)$. Thus the transformation describes a global symmetry, since one is not free to treat different space-time points independently. The infinitesimal transformations of the gluon, ghost and quark fields are given by¶

$$s\Psi \ = \ - igt^a c^a \Psi \ , \tag{2.12}$$

$$sA^a_\mu = D^{ab}_\mu c^b \ , \tag{2.13}$$

$$sc^a \ = \ - \frac{g}{2} f^{abc} c^b c^c \ , \tag{2.14}$$

$$s\bar{c}^a \ = 0, \tag{2.15}$$

where s denotes the Grassmann valued BRST-operator. This operator is nilpotent, *i.e.* $s^2 = 0$. Similar to global gauge symmetry, it is not clear whether the BRST-symmetry generates an unbroken BRST-charge Q_B on the nonperturbative level of the path integral [36, 37]. If so, then the BRST-symmetry of the quantised, gauge fixed theory can be viewed as the analogue to the gauge symmetry of the corresponding classical theory [38].

We are now prepared for a discussion of three interesting ideas related to confinement: the Kugo-Ojima scenario, issues of positivity violations and the Gribov-Zwanziger scenario.

Kugo-Ojima scenario: Confinement denotes the evidence that coloured particles have not been detected directly in an experiment. On the theoretical side this corresponds to the absence of states with non-zero colour charge from the physical part of the asymptotic state space of the theory. A possible mechanism for this property

¶ For brevity I only discuss the so called on-shell transformations.

of QCD has been proposed by Kugo and Ojima [39]. Their scenario is explained in great detail in [40], summaries can be found *e.g.* in [5, 41]. Here I give a brief account omitting details.

The scenario may be phrased in terms of three lines of arguments:

(1.1) If BRST-symmetry is an unbroken symmetry of gauge fixed, nonperturbative QCD, it can be used to define the physical part $\mathcal{W}_{\rm phys}$ of the state space $\mathcal{W}$ of QCD.

(1.2) If the global colour charge is unbroken, it can be shown that $\mathcal{W}_{\rm phys}$ contains colourless states only.

(1.3) The cluster decomposition principle has to be violated in $\mathcal{W}$.

These statements demand some explanations:
Ad (1.1): in covariant gauges one encounters a state space $\mathcal{W}$ that is equipped with an indefinite metric. This state space contains unphysical states (*e.g.* pure ghost or gluon states) as well as physical ones (bound states of quarks and/or gluons). An important step in a proof of confinement is to separate these. To this end Kugo and Ojima suggested to employ the nilpotent BRST charge-operator Q_B, which is well-defined provided BRST-symmetry is unbroken. The physical part $\mathcal{W}_{\rm phys} \subset \mathcal{W}$ of the state space of QCD is then defined to contain exactly those states, which are nontrivially annihilated by Q_B. It can be shown that $\mathcal{W}_{\rm phys}$ has a positive definite metric thus allowing for a probabilistic interpretation of its expectation values.
Ad (1.2): the second line of argumentation concerns the global colour charge. If this charge is well-defined (*i.e.* unbroken), one can show that $\mathcal{W}_{\rm phys}$ contains colourless states only. This suggests that the corresponding asymptotic state space to $\mathcal{W}_{\rm phys}$ represents the observable colour singlet particles. Furthermore it can be shown, that the asymptotic states to the complementary space of $\mathcal{W}_{\rm phys}$ do not contribute to physical S-matrix elements. This so called 'BRST-quartet mechanism' ensures the absence of forward and backward polarised gluons as well as ghost and antighost states from the physical spectrum of the theory[+]. A pedagogical treatment of this mechanism can be found in [29].
Ad (1.3): the cluster decomposition principle has to be violated in the total state space $\mathcal{W}$, but satisfied in $\mathcal{W}_{\rm phys}$. This ensures that all states in $\mathcal{W}_{\rm phys}$ are 'localized' in the sense that one cannot detect possible unphysical components of such a state. Within a meson state, for example, neither the quark nor the antiquark can then be detected individually. Nakanishi and Ojima argued that (1.3) is indeed satisfied within the covariant operator formulation of QCD, see section 4.3.4 of [40].

On the level of Green's functions there are some interesting relations between the statement (1.2) and the infrared behaviour of the propagators of Yang-Mills theory. To understand the structure of this relation better we need to have a closer look on the global colour charge. The corresponding Noether current J^a_μ is given by

$$J^a_\mu = \partial^\nu F^a_{\mu\nu} + \left\{ Q_B, D^{ab}_\mu \bar{c}^b \right\}, \tag{2.16}$$

[+] The corresponding construction in QED is the familiar Gupta-Bleuler formalism.

where $F^a_{\mu\nu}$ is the field strength tensor and Q_B the BRST-charge operator. $D^{ab}_\mu \bar{c}^b$ denotes the covariant derivative of the anti-ghost field. From each of the two terms on the right hand side of (2.16) one can formally define a charge. In the following G^a denotes the charge stemming from the first term whereas N^a denotes the one from the second term. These charges sum up to the global colour charge Q^a:

$$Q^a = G^a + N^a = \int d^3x\, \partial^\nu F^a_{0\nu} + \int d^3x\, \left\{Q_B, D^{ab}_0 \bar{c}^b\right\}. \tag{2.17}$$

Depending on which of the three charges Q^a, G^a and N^a are well-defined or spontaneously broken, Kugo, Ojima and Nakanishi suggested to distinguish three cases [39, 40]:

(i) QED: In the Abelian theory the ghosts decouple and N is always broken. However, G is broken as well due to the presence of massless photons in the field strength tensor $F_{\mu\nu}$. One can then construct a linear combination of N and G such that the massless contributions to both charges cancel. This combination defines an unbroken global colour charge Q.

(ii) Higgs-phase: In the Higgs-phase of the non-Abelian theory one has a vanishing charge G^a for each massive gauge boson (since $\partial^\nu F^a_{0\nu}$ is a total derivative and the integral converges in this case). In these cases N^a is spontaneously broken and therefore Q^a is broken as well.

(iii) Confinement phase: In the confinement phase of non-Abelian gauge theory G^a and N^a should be both unbroken and therefore combine to an unbroken global colour charge Q^a.

The last case is of interest to us. Massless asymptotic contributions to G^a are absent if the nonperturbative transverse gluon propagator is less singular than a simple pole [40]. The charge G^a is then well-defined and vanishes (as a total derivative). Furthermore Kugo showed [42] that the charge N^a is well-defined if the dressed ghost propagator in Landau gauge is more singular in the infrared than a simple pole. Thus these two conditions on the ghost and gluon propagators ensure an unbroken global colour charge Q^a in QCD. This implies that $\mathcal{W}_{\text{phys}}$ contains colourless states only*. Evaluating the infrared properties of the ghost and gluon propagator in Landau gauge thus enables us to test (parts of) the Kugo–Ojima scenario. We will come back to this issue in subsections 2.2 and 2.4.

Positivity violations: The Kugo–Ojima scenario is one particular mechanism that ensures the probabilistic interpretation of the physical states of the quantum theory. However, even if it were eventually shown not to be appropriate, it is apparent that there has to be *some* mechanism which singles out a physical, positive definite subspace in the state space of covariant QCD. This suggests another criterion for confinement, namely violation of positivity. If a certain degree of freedom has negative norm contributions in

* The idea of the proof is easy to see: $\mathcal{W}_{\text{phys}}$ contains only states that are annihilated by Q_B. Furthermore $Q^a = N^a$ is proportional to Q_B. Therefore the expectation value $\langle \text{phys}|Q^a|\text{phys}\rangle$ with $|\text{phys}\rangle \in \mathcal{W}_{\text{phys}}$ vanishes, provided Q_a is well defined.

its propagator, it cannot describe a physical asymptotic state, *i.e.* there is no Källén–Lehmann spectral representation for its propagator. The precise mathematical structure of this condition in the context of an Euclidean field theory has been formulated by Osterwalder and Schrader in the so called axiom of *reflection positivity* [43, 44]. On the level of propagators this condition can be phrased as

$$\Delta(t) := \int d^3x \int \frac{d^4p}{(2\pi)^4} e^{i(tp_4+\vec{x}\cdot\vec{p})}\sigma(p^2) \tag{2.18}$$

$$= \frac{1}{\pi}\int_0^\infty dp_4 \cos(tp_4)\sigma(p_4^2) \;\geq 0\,, \tag{2.19}$$

where $\sigma(p^2)$ is a scalar propagator function extracted from the respective propagator. We will see the consequences of this condition for the gluon and quark propagators in more detail in subsections 2.5 and 3.4.

Gribov-Zwanziger scenario: A third interesting aspect of confinement is a scenario which is related to the gauge fixing procedure. Since problems with gauge fixing are relevant for correlation functions, I discuss these briefly first and state the relation with confinement afterwards. To be specific I choose Landau gauge, since this is the gauge of choice for most of the results discussed in this review. The situation is, however, similar in other gauges as for example Coulomb gauge.

Fixing a gauge completely means singling out one representative configuration from each gauge orbit (2.5). It has been shown by Gribov [45] that the simple Faddeev-Popov procedure is not sufficient in this respect. The Landau gauge condition, $\partial_\mu A_\mu = 0$, generates a hyperplane Γ in gauge field configuration space which still contains gauge field configurations connected by a gauge transformation. These multiple intersection points of a gauge orbit with Γ are called *Gribov copies*, see figure 1 for an illustration (with $\partial_\mu A_\mu$ abbreviated by ∂A). Gribov suggested to get rid of the copies by restricting the hyperplane Γ to the so called *Gribov region* Ω. This is conveniently done by minimising the following L^2-norm of the vector potential along the gauge orbit:

$$F_A(g) := ||A^g||^2 = ||A||^2 - 2i\int d^4x \;\mathrm{tr}(\omega\partial A) + \int d^4x \;\mathrm{tr}(\omega FP(A)\omega) + O(\omega^3), \tag{2.20}$$

with the gauge transformation $g = \exp(i\omega(x))$ and the Faddeev-Popov operator

$$FP(A) = -\partial D(A)^{ab} = -\partial^2\delta^{ab} - g f^{abc}\partial_\mu A^c_\mu. \tag{2.21}$$

Any *local* minimum of this norm implements strictly the Landau gauge condition $\partial A = 0$, and restricts the Faddeev-Popov operator to positive eigenvalues. The Gribov region Ω defined by this prescription has some interesting properties, which are discussed in detail in [46]. Important for us are: (i) Ω contains the origin of the gauge field configuration space and therefore all configurations relevant for perturbation theory and (ii) the lowest eigenvalue of the Faddeev-Popov operator $FP(A)$ approaches zero at the boundary $\partial\Omega$, the *(first) Gribov horizon*. In general, there are still Gribov copies contained in Ω, therefore one needs to restrict the gauge field configuration space even further to the region of global minima of the F_A, which is called *fundamental modular region*. While a restriction to the Gribov region Ω in practical calculations can be achieved with some

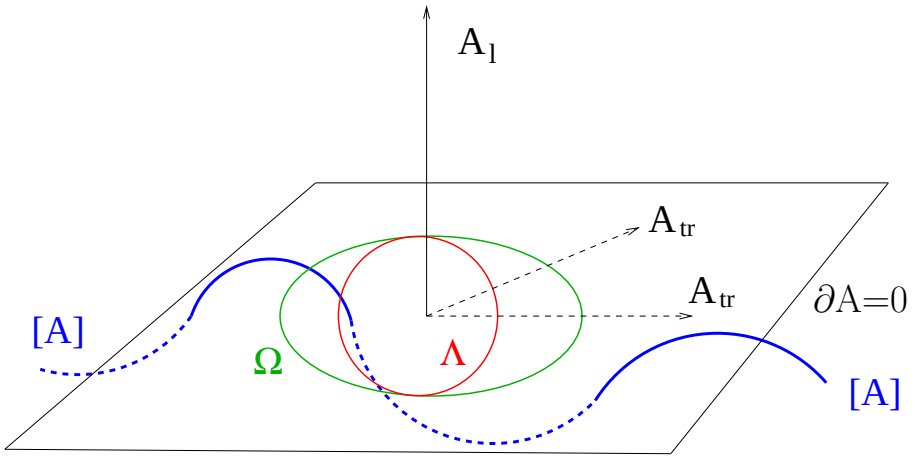

Figure 1. Sketch of the hyperplane Γ in gauge field configuration space obtained by Faddeev-Popov gauge fixing to Landau gauge, $\partial A = 0$. The transverse directions of the gauge field, A_{tr}, generate Γ whereas the longitudinal directions, A_l, are perpendicular to the hyperplane. Shown are furthermore the first Gribov region Ω, and the fundamental modular region Λ containing the trivial configuration $A = 0$. A gauge orbit [A] intersects the hyperplane Γ several times thus generating Gribov copies. The fundamental modular region Λ, however, is intersected only once.

effort, it is extremely cumbersome to identify the configurations of the fundamental modular region. In other words, whereas local minima of F_A are easily found it is almost impossible to identify the global minima. Recent lattice studies [47–57] concentrate some effort on evaluating the size of the problem. For the correlation functions of lattice gauge theory it seems that effects due to Gribov copies are more of quantitative and less qualitative nature. This situation may be even better for the continuum field theory: From an approach using stochastic quantisation Zwanziger argued that Gribov copies inside the Gribov region do not affect the Green's functions of the theory [46]. This is highly fortunate, since a restriction of the generating functional (2.8) to the Gribov region can be implemented in both lattice Monte-Carlo formulations and the DSE approach (see below).

The basic idea of the Gribov-Zwanziger confinement scenario is the statement that gauge field configurations close to the Gribov horizon drive the infrared properties of Yang-Mills theories and are therefore responsible for colour confinement♯. The scenario is probably most directly realized in Coulomb gauge. In this gauge a renormalisation group invariant potential, the colour Coulomb potential, can be identified [45, 58, 59]. This potential is an upper bound for the gauge invariant potential from the Wilson loop. Thus there is no confinement without a confining Coulomb potential [60]. On the other hand, the Coulomb potential is related to an expectation value of the inverse Faddeev-Popov operator. The presence of the Gribov horizon therefore triggers a growing

♯ In fact the relevant configurations should be found close to the common boundary $\partial\Omega \cap \partial\Lambda$ of the Gribov and the fundamental modular region. This is necessary to ensure equality of expectation values on configurations within both regions.

potential and it has been shown that the potential is indeed (almost) linearly rising [61–65].

In Landau gauge no corresponding quantity to the Coulomb potential has been identified so far††. First lattice results for a specific definition of a static quark potential show a flattening out of the potential at large distances, which seems difficult to interpret in the absence of dynamical quarks [65]. This issue remains to be clarified further. There are, however, other infrared effects in Landau gauge which are argued to be driven by the presence of the Gribov horizon:

(I) the presence of the Gribov horizon implies a dressed ghost propagator that is more singular in the infrared than a simple pole [67].

(II) the dressed gluon propagator has to vanish in the infrared [68].

These statements are known as Zwanziger's horizon conditions. They can be viewed as boundary conditions for any solutions of the properly gauge fixed continuum gauge theory. The condition on the ghost is identical to the one encountered in the Kugo–Ojima scenario, whereas the condition on the gluon is stronger than the one discussed above. We will come back to these conditions in subsections 2.2 and 2.5.

At the end of this subsection it is appropriate to give a very brief account on the derivation of Dyson-Schwinger equations from the generating functional of a quantum field theory. To keep the equations simple I will use a very dense, symbolic notation. Readers interested in more details are referred to the textbooks [30, 69] or the reviews [4, 5]. Dyson-Schwinger equations follow from the generating functional (2.8) and the fact that the integral of a total derivative vanishes, *i.e.*

$$\begin{aligned} 0 &= \int \mathcal{D}[A\bar{\Psi}\Psi c\bar{c}]\frac{\delta}{\delta\phi}\exp\left\{-S_{QCD}-S_{gf}+\int d^4x\left(AJ+\bar{\eta}\Psi+\bar{\Psi}\eta+\bar{\sigma}c+\bar{c}\sigma\right)\right\} \\ &= \left\langle -\frac{\delta(S_{QCD}+S_{gf})}{\delta\phi}+j\right\rangle \end{aligned} \tag{2.22}$$

for any field $\phi \in \{A, \Psi, \bar{\Psi}, c, \bar{c}\}$ and its corresponding source $j \in \{J, \eta, \bar{\eta}, \bar{\sigma}, \sigma\}$. Equation (2.22) is valid provided that (i) a representation of the functional integral (2.8) exists and (ii) the measure $\mathcal{D}[A\bar{\Psi}\Psi c\bar{c}]$ is translationally invariant. In the following we will assume that these conditions are satisfied. Furthermore it is important to note that the form of (2.22) does not change when the functional integral is restricted to the Gribov horizon (as required from the discussion above). The reason is that the Faddeev-Popov operator vanishes on the first Gribov horizon. Thus possible boundary terms from restricting the functional integral to the Gribov region vanish [46].

Further functional derivatives of the expression (2.22) with respect to a suitable number of fields ϕ and subsequently setting all sources to zero lead to the Dyson-Schwinger equation for any desired full n-point function. A similar procedure applied to the generating functional $W = \ln(Z)$ or the effective action $\Gamma = W + \langle\phi\rangle j$ leads

†† Although there has been some progress to relate renormalisation group invariants of Landau and Coulomb gauge [66].

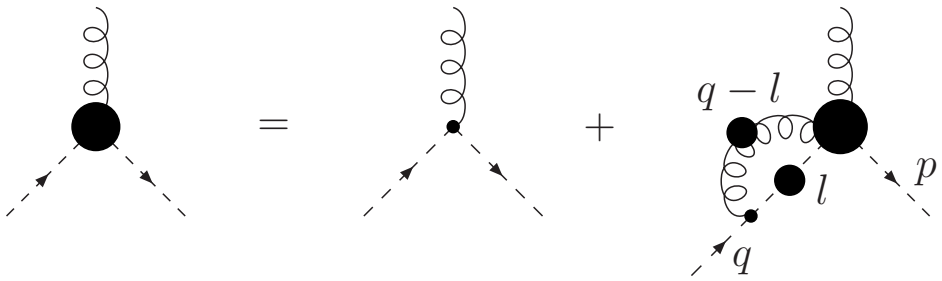

Figure 2. Dyson-Schwinger equation for the ghost-gluon vertex. The filled circles indicate dressed Green's functions, *i.e.* propagators and vertices that contain all effects from quantum fluctuations. A wiggly line denotes a gluon propagator, whereas a dashed line stands for a ghost propagator.

to the DSEs for connected Green's functions and the ones for one-particle irreducible Green's functions. An alternative derivation of DSEs employing Heisenberg's equation of motion and equal time commutation relations can be found in [30]. Conceptual issues and results from Dyson-Schwinger equations in Minkowski-space have been reviewed in [70].

Equation (2.8) and its derivatives constitute an infinite tower of coupled integral equations. In the next subsection we will analyse some of these equations in more detail.

2.2. Infrared exponents of 1PI-Greens functions

The study of infrared exponents of the propagators of Yang-Mills theory has been pioneered by Smekal, Hauck and Alkofer [18, 71] in the late nineties. They were the first to realize an intricate interplay between the ghost and gluon degrees of freedom, which led to the insight that ghosts are dominant in the infrared. These results have been refined since in a number of investigations [19–23, 46, 72–74]. Recently the infrared analysis of Yang-Mills theory has been extended to include the whole tower of DSEs providing selfconsistent scaling laws for one-particle-irreducible (1PI) Green's functions with an arbitrary number of legs [75]. In the following I summarize the general arguments in such an analysis (omitting technical details) and discuss the results. Consequences for the running coupling of Yang-Mills theory are discussed in the next subsection.

The key starting point for an analysis of the infrared behaviour of 1PI-Green's functions is the DSE for the ghost-gluon vertex. This equation is shown diagrammatically in figure 2. On the left hand side we have the dressed ghost-gluon vertex, which can be represented by

$$\Gamma_\mu(q,p) = p_\mu E(p^2,q^2) + (p-q)_\mu F(p^2,q^2). \tag{2.23}$$

Here q, p are the momenta of the incoming and outgoing ghost and colour factors have been omitted. The nonperturbative dressing functions $E(p^2,q^2)$ and $F(p^2,q^2)$ contain all effects from quantum fluctuations. The first diagram on the right hand side of the

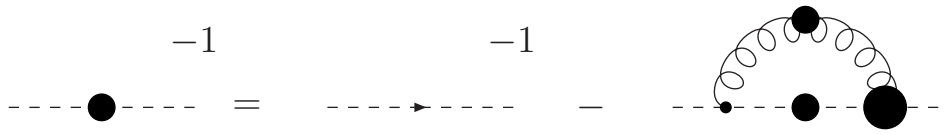

Figure 3. Dyson-Schwinger equation for the ghost propagator. On the left hand side is the inverse of the dressed ghost propagator. On the right hand side we find the inverse of the bare ghost propagator and a loop diagram containing dressed ghost and gluon propagators connected by one bare and one dressed ghost-gluon vertex.

vertex DSE denotes the bare ghost-gluon vertex. It is given by

$$\Gamma^0_\mu(p,q) = \widetilde{Z}_1 p_\mu \,, \tag{2.24}$$

where $\widetilde{Z}_1$ is the vertex renormalisation factor. The second diagram on the right hand side contains a dressed four-point function and a loop with dressed ghost and gluon propagators connected by a bare ghost-gluon vertex. This diagram has an interesting property: In Landau gauge, the momentum q_μ of the incoming ghost factorizes from the diagram. This can be seen directly from figure 2: Since the gluon propagator $D_{\mu\nu}$ is transverse in Landau gauge, its contraction with the bare ghost-gluon vertex $\Gamma^0_\mu = l_\mu$ in the loop of the DSE gives $l_\mu D_{\mu\nu}(l-q) = q_\mu D_{\mu\nu}(l-q)$ and q_μ can be pulled out of the loop integral. Let us assume for the moment that

(A) the loop-integral is finite in the infrared.

(We come back to this assumption in the paragraph below (2.28).) Since q_μ is factorized it is then clear that the dressing loop vanishes if q_μ goes to zero and the ghost-gluon vertex becomes bare in this limit. The same can be shown if p_μ goes to zero. Thus the dressed ghost-gluon vertex in the infrared looks very much like a bare vertex. This astonishing conclusion has been drawn by Taylor long ago [76] and has been confirmed recently by numerical studies of the ghost-gluon vertex on the lattice and in the DSE-approach [74, 77, 78]. Schleifenbaum *et al.* also investigated the mid-momentum behaviour of this vertex and found only moderate structures in the vertex dressing [74].

The simple structure of the ghost-gluon vertex has interesting consequences. Consider the DSE for the ghost propagator, given in figure 3. A bare or finite ghost-gluon vertex at small momenta admits a selfconsistent power law solution in the infrared: Writing the ghost and gluon propagators as

$$\begin{aligned} D^G(p^2) &= -\frac{G(p^2)}{p^2}\,, \\ D_{\mu\nu}(p^2) &= \left(\delta_{\mu\nu} - \frac{p_\mu p_\nu}{p^2}\right)\frac{Z(p^2)}{p^2}\,, \end{aligned} \tag{2.25}$$

one finds power laws for the ghost and gluon dressing functions G and Z with exponents given by† [18, 71]

$$G(p^2) \sim (p^2)^{-\kappa}, \qquad Z(p^2) \sim (p^2)^{2\kappa}\,. \tag{2.26}$$

† This can be checked easily by counting dimensions on both sides of the equation. The loop-integral

The interesting point here is that selfconsistency forces an interrelation of the exponents such that they depend on one parameter κ only. In this notation the Kugo-Ojima criterion (1.2) translates to the condition $\kappa > 0$, which means that the ghost propagator should be more singular and the gluon less singular than a simple pole. Zwanzigers horizon conditions state the same for the ghost propagator, but gives $\kappa > 0.5$ for the gluon dressing function. In a very general analysis of the ghost DSE Watson and Alkofer showed that the exponent κ is positive [20]. The Kugo-Ojima criterion and the horizon condition (I) are therefore satisfied according to this analysis.

The specific value for κ depends on the details of the dressing of the ghost-gluon vertex at small momenta. For a range of possible dressings this has been investigated by Lerche and Smekal in [22]. They argued that $0.5 \leq \kappa < 0.6$ with a possible upper limit given by the result for a bare ghost-gluon vertex, $\kappa = (93 - \sqrt{1201})/98 \approx 0.595$, a value independently found also in [21]. Recent investigations in the framework of exact renormalisation group equations confirm this range [79, 80]. Apart from the lower bound all possible values of κ lead to a vanishing gluon propagator in the infrared in agreement with Zwanzigers horizon condition (II).

On the basis of the relation (2.26) one can also determine the infrared exponents of higher n-point functions. The key idea here is to solve the corresponding DSEs order by order in a skeleton expansion (*i.e.* a loop expansion using dressed propagators and vertices). This program has been carried out by Alkofer, Fischer and Llanes-Estrada in [75]. It turns out that in this expansion the Green's functions can only be infrared singular, if all external scales go to zero. Thus to determine the degree of possible singularities it is sufficient to investigate the DSEs in the presence of only one external scale $p^2 \ll \Lambda_{QCD}^2$, where Λ_{QCD} is of the order of a view hundred MeV. As an example consider the DSE for the three-gluon vertex. In figure 4 we see the full equation as well as an approximation in the lowest order of a skeleton expansion. In the presence of one (small) external scale the approximated DSE has a selfconsistent power law solution given by‡

$$\Gamma^{3g}(p^2) \sim (p^2)^{-3\kappa}. \tag{2.27}$$

The vertex is strongly singular in the infrared. One can see by induction that this solution is also present if terms to arbitrary high order in the skeleton expansion are taken into account. Thus the skeleton expansion is stable wrt. the infrared solution of the DSEs.

This technique can be applied to any other DSE as well. A self-consistent solution

is dominated by momenta of the same magnitude as the external momentum. Thus, for small external momenta one can replace the propagators in the loop by their infrared approximation (2.26). Both sides of the equation are then proportional to $(p^2)^\kappa$.

‡ Again this can be seen by counting anomalous dimensions on both sides of the equations. The loops are dominated by momenta of the same magnitude as the external scale, thus one can substitute the propagators and vertices in the loops by their infrared scaling laws. The leading diagram on the right hand side is the one involving ghosts, diagram (a), the others are less singular (recall $\kappa > 0$). The diagram (a) is proportional to $(p^2)^{-3\kappa}$.

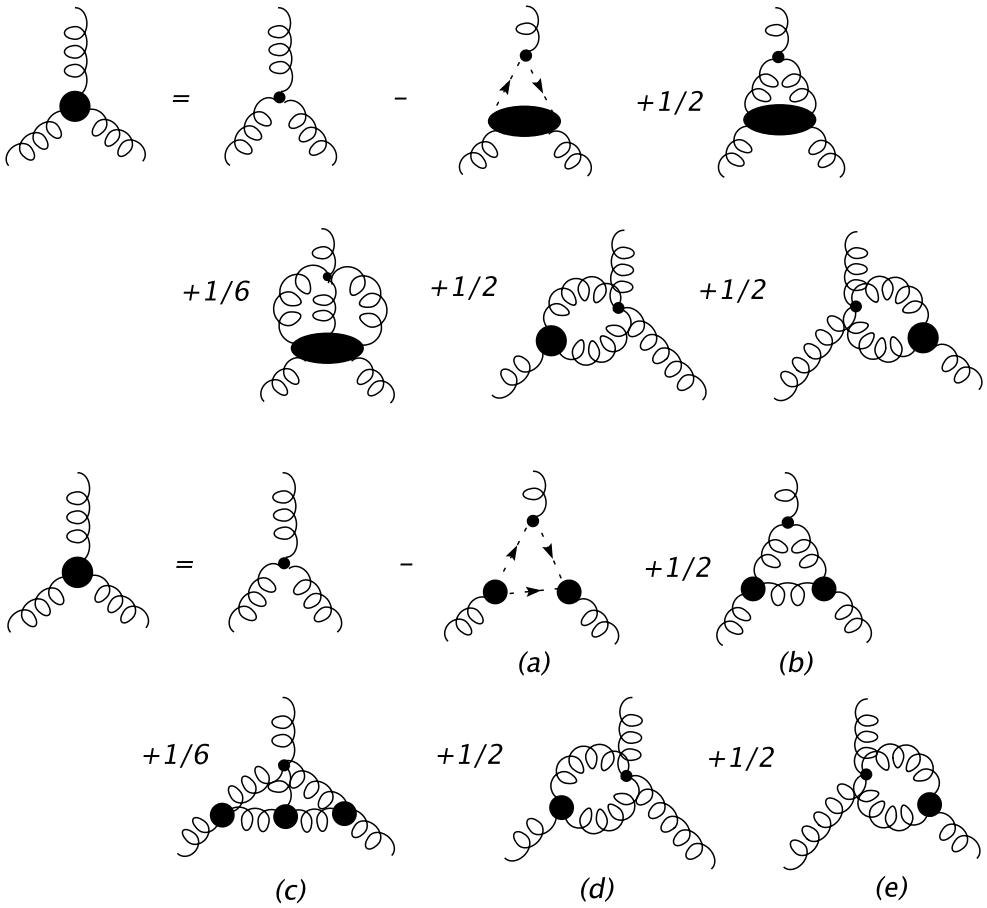

Figure 4. Exact Dyson-Schwinger equation for the three-gluon vertex (upper equation) and lowest order in a skeleton expansion of the four- and five-point functions (lower equation). All internal propagators in the diagrams are to be understood as fully dressed.

of the whole tower of DSEs is then given by [75]

$$\Gamma^{n,m}(p^2) \sim (p^2)^{(n-m)\kappa}. \tag{2.28}$$

Here $\Gamma^{n,m}(p^2)$ denotes the infrared leading dressing function of the 1PI-Green's function with $2n$ external ghost legs and m external gluon legs. By counting anomalous dimensions it can be checked that the expression (2.28) does not only solve the approximated but also the full three-gluon vertex DSE in figure 4 selfconsistently. Furthermore, inserting $\Gamma^{1,2}(p^2) \sim (p^2)^{-\kappa}$ together with the power laws (2.26) into the DSE for the ghost-gluon vertex, figure 2, one can verify the basic assumption **(A)** from the beginning of this subsection: the loop-integral of the vertex dressing is indeed finite in the infrared. Thus (2.28) is a truly selfconsistent infrared solution of the tower of DSEs§.

§ It is worth mentioning that the solution (2.28) also has the correct scaling behaviour such that the Slavnov-Taylor identities of the renormalisation constants are satisfied. Since the theory is multiplicative renormalizable these functions scale with the renormalisation point μ^2 in the same way as

An important aspect of the selfconsistent solution (2.28) is the observation that diagrams containing ghost-loops dominate the infrared behaviour of every DSE. On the level of the generating functional (2.8) this corresponds to the statement that the Faddeev-Popov determinant dominates the quantum fluctuations in the infrared and one can define an infrared asymptotic theory by neglecting the Yang-Mills action, *i.e.* setting $[\exp(-S_{YM})] = 1$ [46]. The solution of this theory is given by the power laws (2.28) (in the presence of only one external scale). Interestingly, this limit is a continuum analogue of the strong coupling limit of lattice gauge theory. It still persists even if quarks are included, as will become clear in subsection 3.2. Zwanziger showed that there is an infinite mass gap in this asymptotic theory [46]. On this basis he suggested a picture of confinement in Landau gauge: Although the infrared modes of the gauge field are suppressed (vanishing gluon propagator), its ultraviolet modes fluctuate wildly because $[\exp(-S_{YM})] = 1$. This causes the decoherence of any field that carries colour; the corresponding particles do not propagate and are therefore confined. In full QCD in Landau gauge it is then the fluctuations of the gauge field around Λ_{QCD} that should be responsible for confinement. Possible candidates for gauge field configurations with this property have been identified in the SU(2)-theory on the lattice: In [26] it was shown that much of the strength of the gluon propagator in this region vanishes if center vortex configurations were eliminated from the statistical ensemble. The reduced ensemble also does not reproduce the linear rising static quark-antiquark potential and is therefore not confining in contrast to the full ensemble including center vortices. A detailed discussion of the confining role of center vortices can be found in [1].

Finally there is caveat: it it necessary to keep in mind that selfconsistency is not enough to establish (2.28) as the 'true' solution of Yang-Mills theory in the infrared. There may be other selfconsistent solutions of the DSEs. In this case one needs other criteria to decide which solution is the one realized in nature. However, besides its relations to confinement there is a further interesting property of the solution (2.28) that qualifies it as a promising candidate: it leads to qualitative universality of the running coupling in the infrared. This is the subject of the next subsection.

2.3. The infrared behaviour of the running coupling

The infrared behaviour of the running coupling of Yang-Mills theory has been investigated in a number of approaches. In the past years evidence is growing that the old picture of 'infrared slavery', *i.e.* the notion of an infrared singular behaviour of the running coupling is not appropriate. Instead, evidence from continuum field theory suggests that the running coupling freezes below a certain momentum scale and develops a fixed point at $p^2 \to 0$. This behaviour has been conjectured from phenomenological investigations (see *e.g.* [81–83] and references therein). It is also found in 'optimized

the 1PI-functions with the external scale p^2. E.g. the relation $Z_1/Z_3 = \widetilde{Z}_1/\widetilde{Z}_3$ between the three-gluon vertex, gluon propagator, ghost-gluon vertex and ghost propagator renormalisation constant leads to $Z_1(\mu^2) = (\mu^2)^{-3\kappa}$, which agrees with (2.27).

perturbation theory' [84] as well as in 'analytic perturbation theory' [85–89]. Certainly, since the infrared limit of QCD is concerned here, genuine nonperturbative approaches seem to be mandatory to underpin these findings. It is therefore quite satisfactory that a fixed point behaviour of the running coupling has also been found in the framework of the exact renormalisation group [79, 80, 90] and from solutions of Dyson-Schwinger equations. In fact the first nonperturbative result stems from Smekal, Hauck and Alkofer within the DSE-approach [71] and has since been elaborated further by Lerche and Smekal [22] and Alkofer, Fischer and Llanes-Estrada [75]. In the following I will first outline what we find from DSEs and then comment on relations to other approaches.

In Landau gauge renormalisation group invariant couplings can be defined from either of the primitively divergent vertices of Yang-Mills-theory, *i.e.* from the ghost-gluon vertex (gh), the three-gluon vertex $(3g)$ or the four-gluon vertex $(4g)$ via

$$\alpha^{gh}(p^2) = \frac{g^2}{4\pi}\, G^2(p^2)\, Z(p^2), \tag{2.29}$$

$$\alpha^{3g}(p^2) = \frac{g^2}{4\pi}\, [\Gamma^{0,3}(p^2)]^2\, Z^3(p^2), \tag{2.30}$$

$$\alpha^{4g}(p^2) = \frac{g^2}{4\pi}\, [\Gamma^{0,4}(p^2)]^2\, Z^4(p^2). \tag{2.31}$$

Here $\Gamma^{0,3}$ denotes the infrared leading dressing of the three-gluon-vertex and $\Gamma^{0,4}$ the corresponding one for the four-gluon vertex. Details on the derivation of these expressions are given in [75]. Note that the multiplicity of the various dressing functions correspond to the multiplicity of the legs of each vertex. Since the ghost-gluon vertex is a finite object in Landau gauge its coupling does not depend on the vertex dressing function. This coupling can therefore be determined from the propagators of Yang-Mills theory alone.

Before we discuss the infrared behaviour of these couplings let us recall some of their general properties. First, it is important to note that the definitions (2.29)-(2.31) correspond to a momentum subtraction scheme (at a symmetric Euclidean momentum point). This entails that couplings from different vertices do not necessarily agree with each other (unlike in the $\overline{MS}$-scheme), but are related via Ward-identities of the renormalisation functions [91, 92]. Although on the one-loop level these differences are rather small [91], to my knowledge there is no argument for this to persist to higher loop order or in the nonperturbative framework discussed here. Second, perturbation theory suggests that the gauge dependence of these couplings is rather weak in the vicinity of Landau gauge. This may be related to the fact that Landau gauge is a fixed point under the renormalisation group flow [93], and justifies Landau gauge as a good starting point for the investigation of these couplings. Below I will comment on corresponding results in a more general class of transverse gauges.

Using the DSE-solution (2.28) in place of the various dressing functions it is easy

to see that all three couplings approach a fixed point† in the infrared [75]:

$$\alpha^{gh}(p^2) = \frac{g^2}{4\pi}\, G^2(p^2)\, Z(p^2) \quad \stackrel{p^2\to 0}{\sim} \frac{c_1}{N_c}\,, \tag{2.32}$$

$$\alpha^{3g}(p^2) = \frac{g^2}{4\pi}\, [\Gamma^{0,3}(p^2)]^2\, Z^3(p^2) \stackrel{p^2\to 0}{\sim} \frac{c_2}{N_c}\,, \tag{2.33}$$

$$\alpha^{4g}(p^2) = \frac{g^2}{4\pi}\, [\Gamma^{0,4}(p^2)]^2\, Z^4(p^2) \stackrel{p^2\to 0}{\sim} \frac{c_3}{N_c}\,. \tag{2.34}$$

They are thus qualitatively universal in the infrared. As explained above, the constants $c_{i=1..3}$ may be different for each coupling and depend in particular on the respective choice of the tensor component used to extract the vertex dressing functions Γ. For the coupling (2.32) of the ghost-gluon vertex this fixed point can be explicitly calculated from the coupled set of DSEs for the ghost and gluon propagator. Employing a bare ghost-gluon vertex Lerche and Smekal found [22]

$$\alpha^{gh}(0) = \frac{2\pi}{3\,N_c} \frac{\Gamma(3-2\kappa)\,\Gamma(3+\kappa)\,\Gamma(1+\kappa)}{\Gamma^2(2-\kappa)\,\Gamma(2\kappa)} \approx 8.92/N_c. \tag{2.35}$$

with $\kappa \approx 0.596$. The dependence of the fixed point on the exponent κ is rather weak. With $0.5 \leq \kappa < 0.6$ one obtains roughly $2.5 < \alpha(0) < 3$ for $N_c = 3$ [22]. The expressions for the other two couplings involve vertex dressing functions which receive contributions from all orders of the (nonperturbative) skeleton expansions of their DSEs (see last subsection). Unfortunately this makes it extremely difficult to determine their fixed point values and no quantitative statement can be made at present.

This result, an infrared fixed point of the running coupling, is interesting for several reasons. The integration over a bounded running coupling is finite, which simplifies the calculation of many observables. Moreover, as discussed *e.g.* in [94], elements of conformal field theory then become relevant at small momentum transfers and commensurate scale relations between different observables hold. These relations link experimental observables to each other without any renormalisation scale or scheme ambiguities. They employ so called *effective charges* [95], which are defined directly from observables. These charges are analytical and non-singular by definition. The couplings (2.29)-(2.31), however, are defined directly from the vertices of the theory. It is thus a highly nontrivial result that they are also non-singular and analytic along the positive Euclidean momentum axis. This certainly suggests some relation between these two types of couplings which would be interesting to clarify in the future. A direct comparison between an effective charge extracted from the Bjorken sum rule and the coupling from the ghost-gluon vertex has been performed in [96]. Both charges have an infrared fixed point and agree well even quantitatively. It is, however, not yet understood

† In the literature the existence of such a fixed point has been attributed frequently to the dynamical generation of a gluon mass, see *e.g.* [88] and references therein. However, from (2.32)-(2.34) we see that this is by no means a necessity. In the language of the infrared exponent κ a gluon mass would correspond to the special case of $\kappa = 0.5$. The mere existence of the fixed points (2.32)-(2.34) however, does *not* depend on any special value of κ. Only its value does, see the discussion around (2.35).

whether this agreement signals a relation between these couplings or whether it is purely accidental.

There is a further interesting aspect on commensurate scale relations. Since they are based on gauge invariant effective charges they hold in any gauge. Thus, if a relation between couplings from the vertices of the theory and effective charges exists, one should find an infrared fixed point for the former type of couplings in other gauges as well. This question has been addressed recently by Fischer and Zwanziger in [66]. We solved the coupled system of DSEs for the ghost and gluon propagator in the infrared in a class of transverse gauges that interpolate between Landau and Coulomb gauge. From the ghost-gluon vertex in these gauges we found two invariant running couplings, which both survive in the Coulomb gauge limit. One of these becomes the colour Coulomb potential. The other coupling indeed has a fixed point in the whole class of transverse gauges including Coulomb gauge. The value of this fixed point is the same as in Landau gauge, $\alpha^{gh}(0) = 8.92/N_c$, for all transverse gauges but the Coulomb gauge limit. A very recent calculation of Schleifenbaum, Leder and Reinhardt finds a substantial increase of this value in the Coulomb gauge limit [97]. It would certainly be interesting to perform a similar analysis for the couplings from the three-gluon and four-gluon vertices. One may hope that there are gauge invariant features (at least within certain classes of gauges) in all couplings defined from the vertices of Yang-Mills theory‡.

2.4. Numerical solutions compared to results from lattice calculations

In the last two subsections we discussed some of the infrared properties of one-particle irreducible Green's functions and related definitions of the running coupling. We are now ready to establish the connection between these results at very small momenta and those known from perturbation theory at large momenta. To this end we will discuss results from numerical solutions to the DSEs, which connect the perturbative and nonperturbative regime. At intermediate momenta these results can be compared to corresponding lattice calculations. We will see that overall both approaches agree well. However, we will also find some interesting differences. In subsection 2.2, we saw that the gluon propagator vanishes in the infrared. Most contemporary lattice calculations obtain a finite propagator at zero momentum. This is an open problem, which is discussed frequently in the literature [55, 100–103]. At the end of this subsection I will outline a possible route towards an explanation of this difference in terms of boundary conditions and finite volume effects on the compact lattice manifold.

The DSEs for the ghost and gluon propagator are given diagrammatically in figure 5. They form a coupled system of equations which demand dressed ghost-gluon, three-gluon and four-gluon vertices as input. Assuming ansaetze for the vertices these equations have been solved selfconsistently for the first time by Smekal, Hauck and

‡ In this respect it is interesting to note that a well-defined class of gauges exists that interpolates also from Landau gauge towards maximal Abelian gauge [98], where confinement may be explained via a dual superconductor scenario. First results on the infrared behaviour of ghost and gluon propagators in these gauges are reported in [99], while results for the coupling are not yet available.

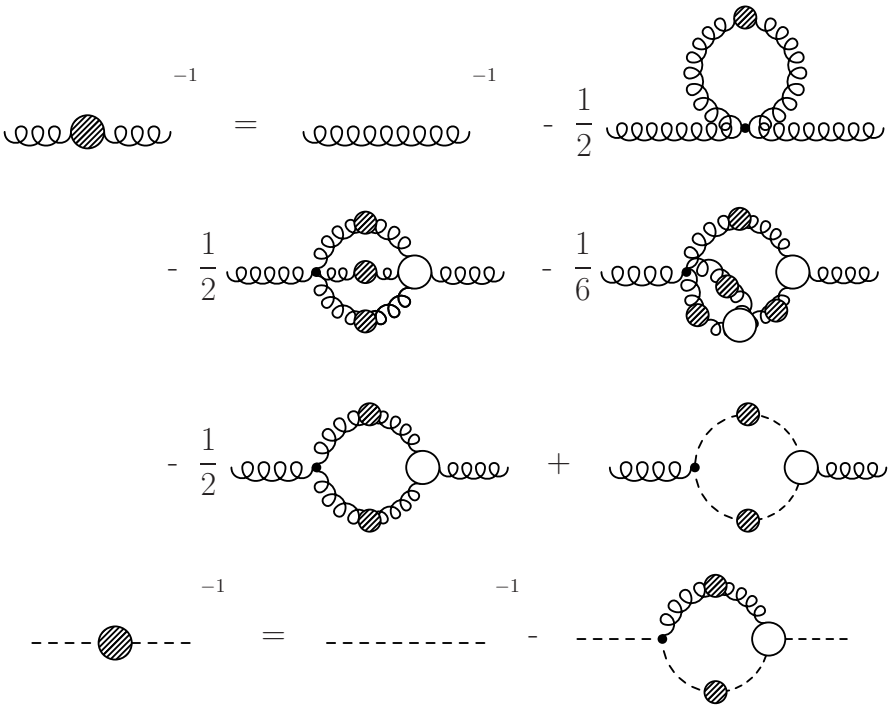

Figure 5. Dyson-Schwinger equations for the gluon and ghost propagator. Filled circles denote dressed propagators and empty circles denote dressed vertex functions.

Alkofer in [18, 71]. Since then numerical techniques have been improved [19] and the technique of angular approximation of loop integrals has been replaced by full fledged numerical integration methods [104–106]. These contemporary solutions still have the same qualitative structure as the ones of [18, 71], but are greatly improved in terms of quantitative reliability.

It is evident that the quality of the solutions of the DSEs depends on the quality of the vertex truncation. The situation is best for the ghost-gluon vertex. Evidence from the analytic infrared analysis (*cf.* subsection 2.2), from lattice calculations (although yet only available for specific kinematics) [77, 78] and a semi-selfconsistent numerical solution of the vertex DSE [74] suggest that a bare vertex approximation is justified. Mild effects from neglecting nontrivial vertex dressing should show up only in the mid-momentum region. This is also the region where the selfinteraction of the gluon is least known. Lattice studies of the three-gluon vertex [107, 108] cover only specific kinematical regions and cannot yet be used to constrain an ansatz for this vertex§. In practise ansaetze for this vertex have been used which agree with the infrared analysis in 2.2. They also lead to the correct behaviour of the propagators in the ultraviolet according to resummed perturbation theory. Contributions involving the four-gluon

§ There is some evidence from the lattice that the vertex is diverging in the infrared [108] as predicted from our infrared analysis in subsection 2.2. However the data do not allow a determination of the precise strength of this divergence.

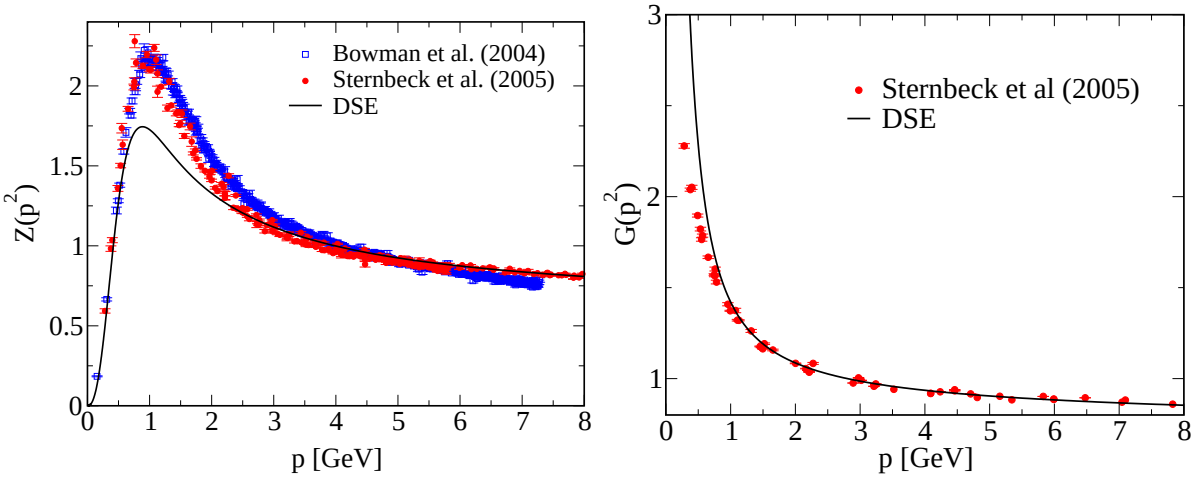

Figure 6. Results for the gluon and ghost propagator from Dyson-Schwinger equations in the continuum compared with recent lattice data. From: Fischer and Alkofer [104] (DSE), Bowman *et al.* [109] (lattice), Sternbeck *et al.* [55]) (lattice).

vertex have been neglected so far‖. While at first sight this last choice might seem arbitrary, it is in fact well justified from the infrared analysis in subsection 2.2: the gluon two-loop diagrams are subleading in the infrared. They are also subleading in the ultraviolet, since they do not appear to leading order in perturbation theory. In the intermediate momentum regime such a truncation together with uncertainties in the dressing of the three-gluon and ghost-gluon vertex introduces quantitative errors. These have to be controlled a posteriori by a comparison of the results for the gluon and ghost propagator with corresponding lattice calculations.

Such a comparison can be seen in figure 6. The global structure of the solutions in both the lattice and the DSE approach is the same. In the ultraviolet all solutions reproduce perturbation theory as expected (this can be shown analytically for the DSEs). In the intermediate momentum region one observes a larger bump in the gluon dressing function from the lattice compared to the DSE result. This difference serves as an estimate of the neglected effects due to the gluon selfinteraction. In the infrared both approaches seem to agree nicely on a linear plot. The numerical results from the DSEs agree here with the analytical results discussed in subsection 2.2 (this can be seen best on a log-log plot, displayed *e.g.* in [104]) and the lattice data are not far away. However, we have to look closer here.

In figure 7 we see the same results displayed differently. Plotted is the gluon propagator $Z(p^2)/p^2$ instead of the dressing function $Z(p^2)$. The ghost dressing function $G(p^2)$ is shown on a log-log plot. In the infrared we clearly see differences now. The ghost dressing function in figure 7 diverges in the infinite volume/continuum limit, whereas it

‖ A first attempt to include the gluon two-loop diagrams has been made in [105]. However, the employed ansaetze for the three- and four-gluon vertices disagree with the requirement of selfconsistency in the vertex DSEs. Unfortunately this sheds some doubt on the conclusiveness of the results achieved there.

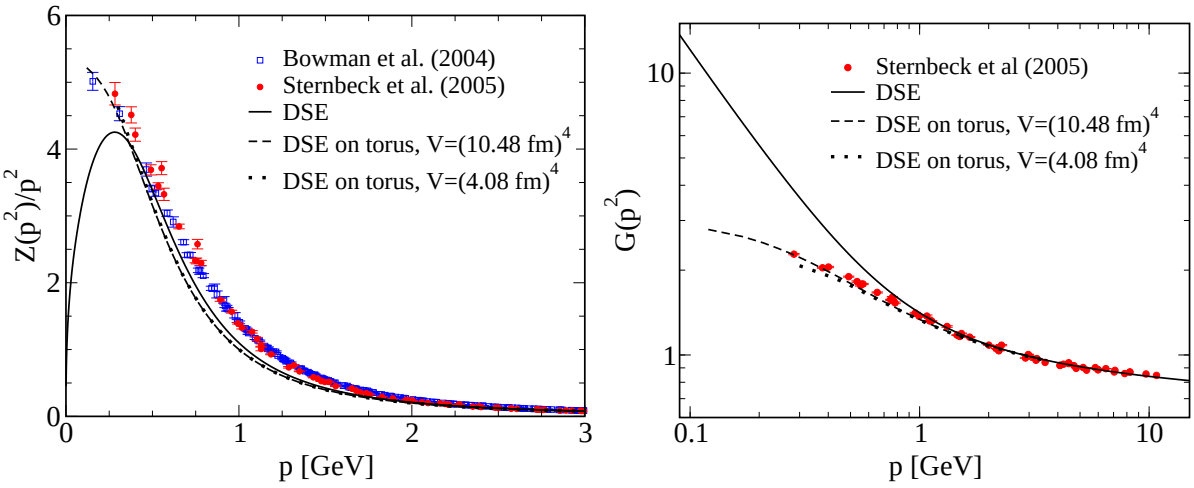

Figure 7. Same results as in figure 6 but displayed differently. In addition results from DSEs on a torus are shown. From: Fischer and Pennington, [110] (DSE on torus).

stays finite on the lattice, *i.e.* on the compact manifold. For the gluon propagator, the differences can be expressed in terms of the infrared power law,

$$Z(p^2) \sim (p^2)^{2\kappa}. \tag{2.36}$$

One obtains $\kappa \approx 0.5$ (IR-finite) on a compact manifold, whereas $\kappa \approx 0.6$ (IR-vanishing) on R^4 in agreement with the analytical results (*cf.* subsection 2.2)¶. This is a decisive difference, since it can be shown that an infrared vanishing gluon propagator cannot have a positive definite spectral function and is therefore confined, see next subsection. Indeed, Zwanziger has argued that the lattice gluon propagator should vanish in the continuum limit [68], *cf.* subsection 2.1. However, no statement could be made as to the rate with which the continuum limit behaviour is approached. Current extrapolations of lattice data to the infinite volume limit are under discussion [25, 101, 103, 112, 113].

As an attempt to clarify this situation we changed the base manifold on our DSEs from R^4 to the lattice manifold, *i.e.* a torus with periodic boundary conditions [100, 114]. The vertex truncation is the same as for the R^4-case, such that we could compare solutions on a box with a known infinite volume/continuum limit. The result is also shown in figure 7. We obtained ghost and gluon propagators on the box which are qualitatively similar to the lattice results. Moreover, by varying the volume of the box we found that the volume dependence of these solutions is very weak, so that the infinite volume/continuum limit is approached extremely slowly. Thus it seems as if there is a genuine difference between propagators on different manifolds. Since there are indications [79] that the 'true' exponent κ may be closer to $\kappa \approx 0.5$ and therefore closer to the current lattice data than our value $\kappa \approx 0.596$, the differences shown in figure 7 may serve as a measure of the upper limit of these effects.

¶ The only recent numerical DSE-study that finds an infrared finite gluon propagator also in the continuum is reported in [111]. This study, however, is hardly conclusive, since it employs a (highly

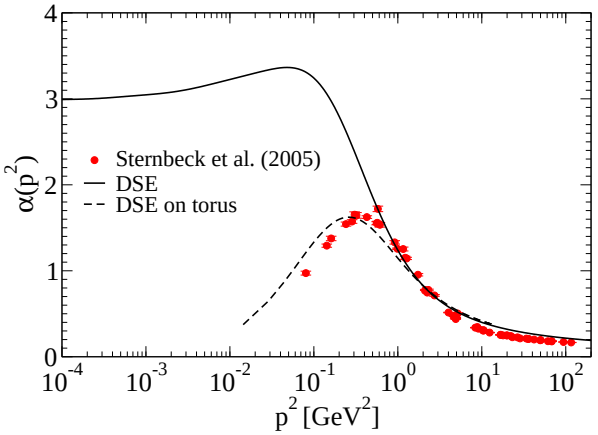

Figure 8. Results for the running coupling of the ghost-gluon vertex from DSEs in the continuum and on the torus compared to lattice data. From: Fischer and Alkofer [104]) (DSE), Fischer and Pennington [110] (DSE on torus), Sternbeck *et al.* [55] (lattice).

The running coupling resulting from the ghost and gluon dressing functions of figure 7 is shown in figure 8. In the continuum solution we observe a fixed point in the infrared, which corresponds to the analytic value (2.35). The results from DSEs on a compact manifold and the lattice show an infrared vanishing coupling[+]. Although the quantitative agreement between the DSE-solution on the torus and the lattice data may well be accidental, the qualitative agreement suggests that finite volume and boundary effects may play an important role for the infrared behaviour of the running coupling.

The running coupling as it results from numerical solutions for the gluon and ghost propagators can be accurately represented by [115]

$$\alpha_{\rm fit}(p^2) = \frac{1}{1+(p^2/\Lambda^2_{\rm QCD})}\left[\alpha_S(0) + (p^2/\Lambda^2_{\rm QCD})\frac{4\pi}{\beta_0}\left(\frac{1}{\ln(p^2/\Lambda^2_{\rm QCD})} - \frac{1}{p^2/\Lambda^2_{\rm QCD}-1}\right)\right], \quad (2.37)$$

with $\beta_0 = (11N_c - 2N_f)/3$ and the probably unphysical bump in the coupling at 500 MeV has been omitted. The form of the cancellation of the Landau pole at $p^2 = \Lambda^2_{\rm QCD}$ is reminiscent of analytic perturbation theory [85]. The expression (2.37) is analytic in the complex p^2 plane except on the real timelike axis where the logarithm produces a cut. This brings us to our next topic: the analytical structure of the gluon propagator.

2.5. The analytical structure of the gluon propagator

An important problem in quantum field theory is the question of the separation of physical and unphysical degrees of freedom. In linear covariant gauges, where the state space of QCD necessarily is equipped with an indefinite metric this question is related to the task of specifying a physical, positive definite subspace $\mathcal{W}_{\rm phys}$, as discussed in subsection 2.1. BRST symmetry and the consequential BRST quartet mechanism serve to show that longitudinal gluon and ghost states are orthogonal to all states in $\mathcal{W}_{\rm phys}$

dubious) renormalisation prescription that enforces the propagator to be constant in the infrared.

[+] A similar result has been reported for the coupling from the three-gluon vertex on the lattice in [102].

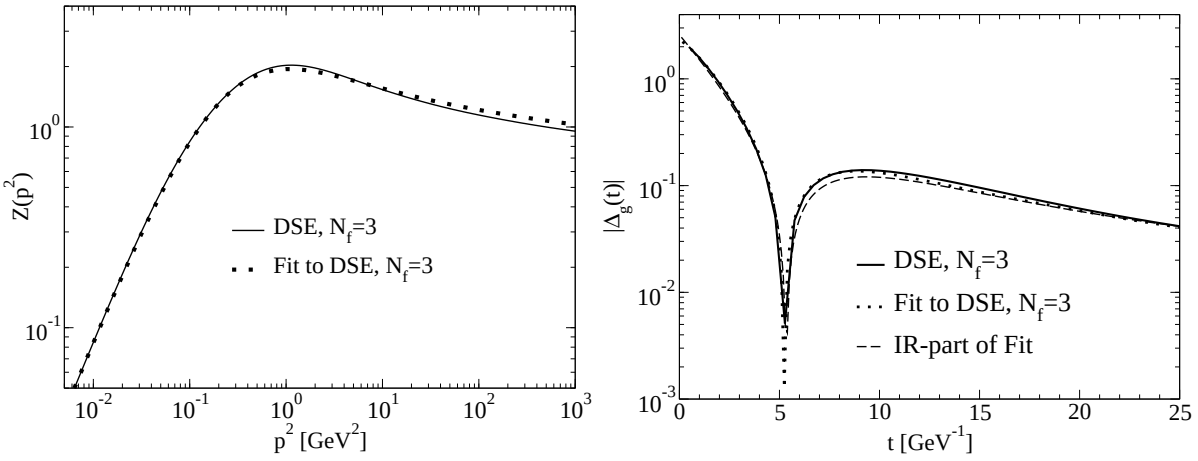

Figure 9. Left: The DSE-result for the gluon dressing function and the fit (2.39) are shown. Right: The corresponding Schwinger functions (absolute value) of the propagator and the fit. From: Alkofer, Detmold, Fischer and Maris [116].

and therefore do not contribute to physical S-matrix elements. However, this is not automatically guaranteed for transverse gauge bosons. In fact, transverse, massive gauge bosons are physical particles in the Higgs phase of Yang-Mills theory. Thus one has to understand the details of the mechanism by which transverse gluons are taken out of the spectrum in the confined phase.

The question whether the gluon propagator is infrared finite or vanishing is decisive in this context. This can be seen easily as the relation,

$$0 = D(p=0) = \int d^4x \; \Delta(x)\,, \tag{2.38}$$

(with $D(p) = Z(p^2)/p^2$) implies that the propagator function in coordinate space, the Schwinger function $\Delta(x)$, must contain positive as well as negative norm contributions, with equal integrated strengths. Thus if the transverse propagator is vanishing in the infrared, (2.38) immediately tells us that transverse gluons cannot be part of the positive definite, physical state space of Yang-Mills theory. The generation of infrared power laws with $\kappa > 0.5$ is therefore a viable candidate for a mechanism of gluon confinement [22, 46, 71, 116].

The analytic structure of the gluon propagator has been explored in [116]. The idea is to fit the numerical solutions for the propagator function $D(p^2) = Z(p^2)/p^2$ (shown in figure 6) with an analytic expression such that the Fourier transform of the fit also reproduces the Fourier transform of the propagator given in (2.19). Very good agreement is obtained with the fit form

$$Z_{\rm fit}(p^2) = w \left(\frac{p^2}{\Lambda_{\rm QCD}^2 + p^2} \right)^{2\kappa} \left(\alpha_{\rm fit}(p^2) \right)^{-\gamma} , \tag{2.39}$$

with $w = 2.65$ and $\Lambda_{\rm QCD} = 520$ MeV. The overall magnitude, w, depends only on the renormalisation scale. The ultraviolet anomalous dimension $\gamma = (-13N_c + 4N_f)/(22N_c - 4N_f)$ of the gluon propagator corresponds to one-loop resummed perturbation theory.

The infrared exponent, κ, is determined from the infrared analysis, *cf.* subsection 2.2. The expression for the running coupling, $\alpha_{\rm fit}(p^2)$, has been given in (2.37). Thus the parameterisation of the gluon propagator has effectively only one parameter, the scale $\Lambda_{\rm QCD}$ where the dressing function turns over from the infrared power law behaviour towards the ultraviolet logarithmic running. The analytic structure of the fit can nicely be interpreted: The discontinuity across the cut in $Z_{\rm fit}(p^2)$, which vanishes for $p^2 \to 0^-$, diverges to $+\infty$ at $p^2 = -\Lambda_{\rm QCD}^2$ on both sides and drops again to zero for $p^2 \to -\infty$. This cut can be interpreted as the possible decay of the transverse gluon into a ghost-antighost pair or into two or three nonperturbative gluons.

Both the propagator and its fit are shown in figure 9 (shown are the unquenched results which are discussed further in subsection 3.2). The Schwinger function, $\Delta_g(t)$, based on the fit (2.39) is compared to the DSE solution in the right diagram of figure 9. To enable a logarithmic scale, the absolute value is displayed. In both diagrams the agreement of the numerical solutions with the fit is excellent. This gives some confidence that at least on a qualitative level the analytic properties of the Landau gauge gluon propagator are uncovered by the fit. The Schwinger function $\Delta_g(t)$ has a zero for $t \approx 5\,\mathrm{GeV}^{-1} \approx 1\,\mathrm{fm}$ and is negative for larger Euclidean times. Thus one clearly observes positivity violations in the DSE gluon propagator at the expected scale for confinement. This scale is related to the position of the bump in the gluon propagator and therefore to the position of the breakdown of the infrared asymptotic theory discussed in subsection 2.2. This underpins the abovementioned suggestion by Zwanziger that fluctuations at a scale of Λ_{QCD} trigger confinement in Landau gauge.

3. Dynamical chiral symmetry breaking

Quarks are the central building blocks for mesons and baryons and provide their primary quantum numbers. In this context chiral symmetry and its breaking pattern are of great importance in our understanding of the structure and the spectra of light mesons and baryons. Most of the mass of these objects is generated dynamically, as we will see in detail later on.

Similar to the situation in the Yang-Mills sector there is an interesting interplay between the Dyson-Schwinger approach and lattice simulations. Since the strengths and weaknesses of both approaches are complementary, it is fruitful to combine both methods to explore the details of chiral symmetry breaking in QCD.

In principle, the lattice is an appropriate nonperturbative tool to study the effects of dynamical chiral symmetry breaking. Lattice actions implementing overlap, domain wall or perfect fermions obey the Ginsparg-Wilson relation, which ensures that a lattice variant of chiral symmetry is satisfied. In practice, however, lattice simulations with reasonably small quark masses are extremely expensive in terms of CPU-time. It is only with staggered fermion actions that quark masses not too far from their physical values have been achieved to date. However, these actions have the disadvantage that full chiral symmetry is only recovered in the continuum limit and there is no certainty

with any finite volume that the correct breaking pattern can be observed [2].

Dyson-Schwinger equations offer a suitable alternative method to investigate the effects of dynamical chiral symmetry breaking. Since the method is formulated in continuum field theory no finite volume effects are present in the first place (see however subsection 3.3 for results on a compact manifold). Moreover, arbitrarily small quark masses can be implemented and the chiral limit can be directly investigated without any need for extrapolations. Via the quark propagator one has direct access to the chiral condensate, the order parameter of dynamical chiral symmetry breaking. The truncations in the quark DSE, however, have to be controlled. This can be done by comparison with lattice results at quark masses feasible on the lattice.

In the last section I summarized some results on the structure of Yang-Mills theory, that have been discovered in the past years. We are now ready to discuss the impact of these results on the quark sector of QCD. I will first summarize some properties of the quark propagator in quenched approximation, before I consider the backreaction of the quarks on the Yang-Mills sector of QCD in subsection 3.2 and compare to corresponding lattice results. This comparison will be extended in subsection 3.3, when I discuss a formulation of the quark DSE on a compact manifold. As a byproduct of this investigation we will see that a minimal volume for chiral perturbation theory (and chiral symmetry breaking on the torus in general) can be obtained from the DSEs. The section ends with a short discussion of the analytical properties of the quark propagator.

3.1. Quark DSE and quark-gluon vertex

The renormalized Dyson-Schwinger equation for the dressed quark propagator $S(p)$ is given by

$$S^{-1}(p) = Z_2\, S_0^{-1}(p) + g^2\, Z_{1F}\, C_F \int \frac{d^4q}{16\pi^4}\, \gamma_\mu\, S(q)\, \Gamma_\nu(q,k)\, D_{\mu\nu}(k)\,, \qquad (3.1)$$

with the momentum routing $k = q - p$. Here $D_{\mu\nu}$ denotes the dressed gluon propagator, $\Gamma_\nu(q,k)$ the dressed quark-gluon vertex and $S_0(p)$ the bare quark propagator. Z_2 and Z_{1F} are renormalisation factors of the quark propagator and the quark-gluon vertex. The factor $C_F = (N_c^2 - 1)/2N_c$ stems from the colour trace of the loop. All dependences of the renormalisation point are treated implicitly. A diagrammatical representation of this equation is given in figure 10.

The dressed quark propagator can be written as

$$S(p) = \frac{1}{-i\not{p}\, A(p^2) + B(p^2)} = Z_f(p^2) \frac{i\not{p} + M(p^2)}{p^2 + M^2(p^2)}\,, \qquad (3.2)$$

where $A(p^2)$ and $B(p^2)$ are the vector and scalar dressing functions of the quark. The inverse $Z_f(p^2) = 1/A(p^2)$ of the vector dressing function is also called the quark wave function renormalisation. The ratio

$$M(p^2) := B(p^2)/A(p^2) \qquad (3.3)$$

is the quark mass function. It is important to note that the dependence of $A(p^2)$ and $B(p^2)$ on the renormalisation point μ^2 cancels out in the ratio (3.3). The quark mass

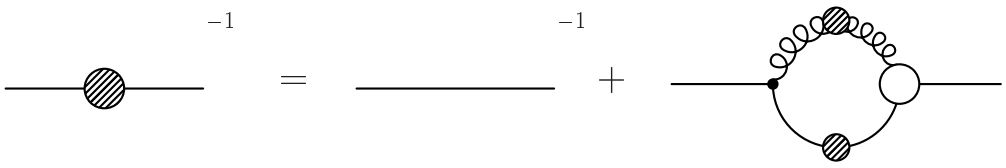

Figure 10. A diagrammatical representation of the quark Dyson-Schwinger equation. On the left hand side we find the inverse dressed quark propagator. The diagrams on the right hand side denote the inverse bare propagator and a dressing loop containing dressed quark and gluon propagators and one bare and one dressed quark-gluon vertex.

function is therefore a renormalisation group invariant. The bare quark propagator is given by

$$S_0(p) = \frac{1}{-i\not{p} + Z_m\, m_R} \tag{3.4}$$

and contains the renormalised 'current quark mass' m_R and the mass renormalisation factor Z_m.

The two tensor structures in the quark propagator, $\not{p}$ and 1, behave different under chiral symmetry transformations. The vector part $\not{p}$ is invariant, whereas the scalar part is not. A nonvanishing function $B(p^2)$ signals unambiguously that chiral symmetry is broken and therefore may serve as an order parameter. Since $B(p^2)$ is determined by the quark DSE (3.1), this equation is also called the *gap equation* of QCD. Another order parameter for dynamical chiral symmetry breaking is the chiral condensate. It can be shown analytically [117] that the ultraviolet behaviour of the quark propagator in the chiral limit $Z_m\, m_R \to 0$ can be described by†

$$M(p^2) = \frac{2\pi^2\gamma_m}{3} \frac{-\langle\bar{\Psi}\Psi\rangle}{p^2\left(\frac{1}{2}\ln(p^2/\Lambda^2_{QCD})\right)^{1-\gamma_m}}\,. \tag{3.5}$$

Here $\gamma_m = \frac{12}{11N_c - 2N_f}$ is the anomalous dimension of the quark and $\langle\bar{\Psi}\Psi\rangle$ denotes the renormalisation point independent chiral condensate. This condensate is related to the renormalisation point dependent condensate from the trace of the quark propagator.

$$-\langle\bar{\Psi}\Psi\rangle(\mu^2) := Z_2(s,L)\, Z_m(s,L)\, N_c\, \mathrm{tr}_D \int \frac{d^4q}{(2\pi)^4} S_{ch}(q^2,s)\,, \tag{3.6}$$

by a simple logarithmic factor

$$\langle\bar{\Psi}\Psi\rangle(\mu^2) = \left(\frac{1}{2}\ln(\mu^2/\Lambda^2_{QCD})\right)^{\gamma_m} \langle\bar{\Psi}\Psi\rangle\,, \tag{3.7}$$

provided the renormalisation point μ^2 is taken large enough. The trace tr_D in (3.6) is over Dirac indices and S_{ch} denotes the quark propagator in the chiral limit. Thus there are two ways to extract the chiral condensate from S_{ch}: either by performing a fit to the ultraviolet tail of the mass function or from evaluating (3.6) numerically. Both procedures agree with each other.

† The relation of this expression to the Banks-Casher equation is discussed by Langfeld *et al.* in [118].

The two external ingredients in the quark DSE (3.1) are the gluon propagator and the quark-gluon vertex. While the nonperturbative gluon propagator is a well known object by now (*cf* section 2), it is the nonperturbative structure of the quark-gluon vertex which is at the focus of contemporary studies. This vertex can be decomposed in a basis of twelve tensor structures‡

$$\Gamma_\mu = ig \left(\sum_{i=1}^{4} \lambda_i L_\mu^i + \sum_{i=1}^{8} \tau_i T_\mu^i \right) . \tag{3.8}$$

Most of the properties of the nonperturbative dressing of these structures are not even qualitatively known. Contemporary lattice studies of the vertex [120] still have large error bars and cannot uncover the infrared properties of the vertex. It is well known, however, that sizeable dressing effects have to be present. A bare quark-gluon vertex is not capable to trigger dynamical chiral symmetry breaking. This result underlines the fact that dynamical chiral symmetry breaking is an entirely nonperturbative phenomenon. The necessary interaction strength in the vertex could be concentrated in the (perturbatively) leading structure

$$L_\mu^1 = \gamma_\mu \, , \tag{3.9}$$

or it could be distributed among several tensor components. One of the potentially important other components of the vertex is the scalar piece,

$$L_\mu^3 = i(p_1 + p_2)_\mu \, , \tag{3.10}$$

which is proportional to the sum of the incoming and outgoing quark momenta p_1 and p_2. This structure is not invariant under chiral transformations in contrast to the leading γ_μ-part of the vertex. It only appears when chiral symmetry is broken dynamically and provides then a significant self-consistent enhancement of dynamical chiral symmetry breaking in the quark DSE [115].

Basically there have been two different strategies to assess the quantitative impact of different tensor structures of the vertex on the quarks. First, ansaetze for the vertex have been constructed that satisfy approximate forms of the Slavnov-Taylor identity for the quark-gluon vertex and avoid kinematical singularities [115]. Second, a number of attempts have been made to determine parts of the vertex from solutions to approximate forms of the vertex DSE [11, 121–123]. To date the latter approach has not yet reached the state of selfconsistency, but seems to be promising for the future. In this review I focus on the first strategy.

The Slavnov-Taylor identity (STI) for the (colour stripped) ghost-gluon vertex $\Gamma_\nu(q,k)$ is given by [124]

$$G^{-1}(k^2)\, k_\nu\, \Gamma_\nu(q,k) = S^{-1}(p)\, H(q,p) - H(q,p)\, S^{-1}(q), \tag{3.11}$$

where q and p are the quark momenta. This identity connects the vertex to the quark propagator $S(p)$ and the ghost-quark scattering kernel $H(q,p)$. The presence of the

‡ There are three independent four vectors: γ_μ, p_μ and q_μ, and four types of scalars: 1, $\not{p}$, $\not{q}$, $[\not{p},\not{q}]$. Combined together these enumerate to twelve independent tensor structures [119].

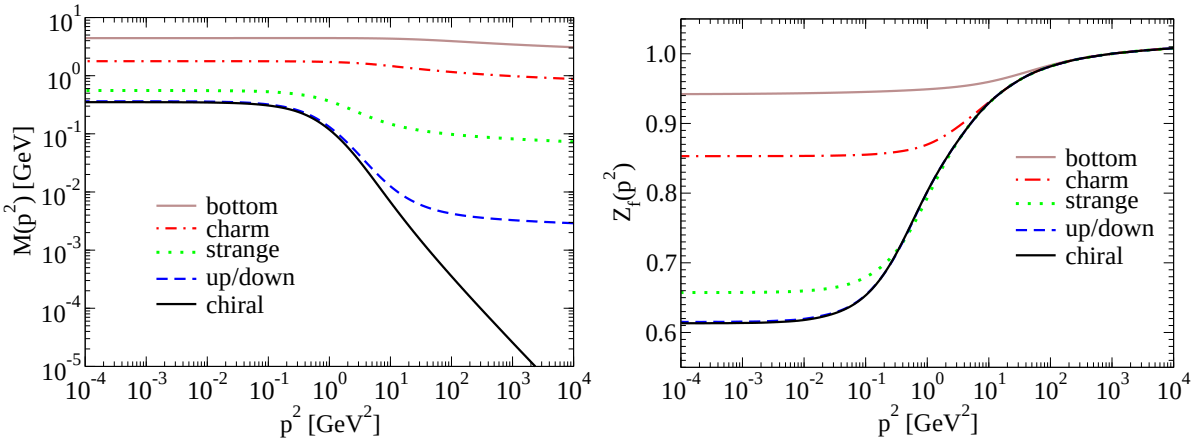

Figure 11. Results for the quark mass function $M(p^2)$ and the wave function $Z_f(p^2)$ from the quark DSE for various physical current quark masses. Based on: Fischer and Alkofer [115].

ghost dressing function $G(k^2)$ in the STI tells us that the vertex may be an infrared singular object similar to the three- and four-gluon vertices [75] (*cf.* subsection 2.2). An explicit ansatz for the quark-gluon vertex built along this identity has been constructed in [115]. Its most important parts read

$$\Gamma_\nu(q,k) \sim G^2(k) \left[\frac{A(p)+A(q)}{2}\gamma_\nu + i\frac{B(p)-B(q)}{p^2-q^2}(p+q)_\nu + (\ldots) \right], \quad (3.12)$$

i.e. it contains a vector as well as a scalar part with relative strength given by the Abelian approximation to the STI (3.11). With this vertex ansatz and numerical solutions for the ghost and gluon propagators the quark DSE is closed and can be solved numerically.

Results for realistic quark masses can be seen in figure 11. By comparison of the quark mass function of a light (up/down) quark with the chiral limit we see that virtually all of the infrared mass of the up/down quark is generated dynamically. These objects are thus dominated by effects due to dynamical chiral symmetry breaking. Dynamical effects are still large for the strange quark. However, already the charm quark and certainly the bottom quark are more or less static objects in the sense that dynamical effects are overwhelmed by the large current quark mass and its evolution according to the renormalisation group.

For the quark wave function $Z_f(p^2)$ a large fraction of dynamical mass is signalled by the size of the dip in the infrared. Whereas the wave function for the up-quark is a nontrivial object it becomes more and more static the heavier the quarks are. In general we see that the DSE-solutions naturally connect the nonperturbative infrared with the perturbative ultraviolet momentum region. What appears as a 'current quark' at large momentum transfer and as a 'constituent quark' at small momenta is described by the very same object: the dressed quark propagator.

At large momenta the quark mass functions scale logarithmically with momentum according to their expected behaviour from resummed perturbation theory (this can be shown analytically in the quark DSE [117]). In the chiral limit, where this logarithm is

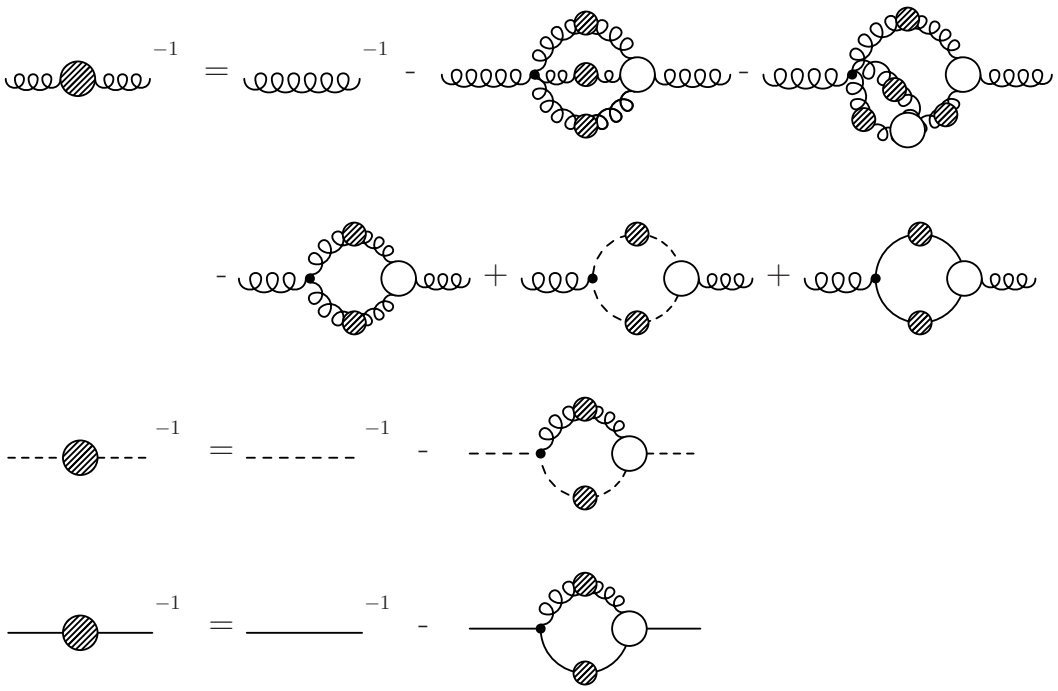

Figure 12. The coupled set of Dyson-Schwinger equations for the ghost, gluon and quark propagators. (The tadpole diagram in the gluon DSE has been omitted, since it drops out in the process of renormalisation.)

absent, one can directly observe the asymptotic behaviour (3.6) and extract the chiral condensate. The most recent value for the condensate from the DSE-approach (with a lattice based interaction, see subsection 3.3) is given by [110]

$$-\langle\bar{\Psi}\Psi\rangle^{\overline{MS}}(\mu^2) \;=\; (253.0 \pm 5.0\mathrm{MeV})^3, \tag{3.13}$$

employing $\Lambda_{QCD}^{\overline{MS}} = 0.225(21)$MeV [125]. The quoted error combines numerical and scale errors but does not include systematic errors due to the approximation of the quark-gluon vertex. It is therefore interesting to compare the central value with recent results from the lattice. Gimenez *et al* [126] find $(265 \pm 27\mathrm{MeV})^3$ from an operator product expansion employing an $O(a)$-improved quenched Wilson action. Wennekers and Wittig [127] quote $(285 \pm 9\mathrm{MeV})^3$, determined from a quenched overlap action. Given that systematic uncertainties exist in all three approaches one can say that the values are in fair agreement with each other.

3.2. Unquenching effects

Unquenching is expected to have a significant impact on the properties of QCD if the number of fermion flavours N_f is large. QCD ceases to be asymptotically free for a sufficiently large number of flavours N_f. Furthermore a chiral phase transition to the symmetric phase is expected. However, the critical N_f are expected to be of $\mathcal{O}(10)$§,

§ A recent calculation of Gies and Jäckel in the framework of the exact renormalisation group results in a critical number of flavours of $N_f^c = 10.0 \pm 0.4$ for the chiral transition [128].

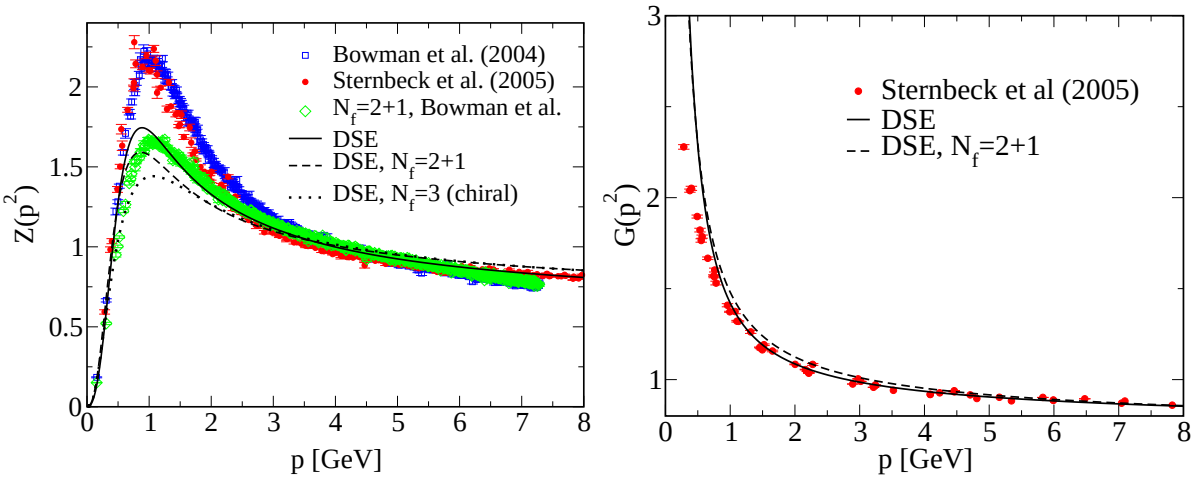

Figure 13. Unquenched gluon and ghost propagators compared to quenched results. For the ghost propagator unquenched lattice data are not yet available. From: Fischer and Alkofer [115] (DSE), Bowman *et al.* [109] (lattice), Sternbeck *et al.* [55]) (lattice).

which is large compared to the physical case of three light flavours. Realistic effects due to unquenching may therefore be not too large.

For the ghost, gluon and quark propagators of QCD these effects have been determined recently in the DSE-approach [106, 115]. The effects in the gluon propagator have since been confirmed on the lattice [109, 129, 130]; no unquenched lattice results for the ghost propagator are available yet. In the Dyson-Schwinger approach one solves the coupled set of three equations, which includes a quark loop in the gluon DSE, see figure 12 for a diagrammatical representation. Compared to the case of pure Yang Mills theory, figure 5, there is an additional quark-loop in the gluon DSE. This has some impact on the intermediate momentum region as can be seen from the numerical results shown in figure 13. In the region around 1 GeV enough energy is present to generate dynamical quark-antiquark pairs from the vacuum. These provide some colour screening, which partly eliminates the antiscreening effects from the gluon self interaction. Consequently the bump in the gluon dressing function decreases. This effect is clearly present in both the DSE and the lattice study. In the chiral limit the screening effect of the quark loop becomes stronger as the energy needed to create a quark pair from the vacuum becomes smaller with decreasing bare quark mass. In the ultraviolet momentum region unquenching effects are only visible in modified anomalous dimensions as expected from resummed perturbation theory.

It is, however, important to note that the inclusion of three light flavours has no effect on the infrared structure of the Yang-Mills part of QCD. This can be understood easily in terms of our infrared analysis from subsection 2.2. Quark loops in the Yang-Mills sector contain at least two massive quark propagators, which are proportional to $[p^2+M(p^2)]^{-1}$. Provided chiral symmetry is broken dynamically we always have sizeable quark masses in these propagators that dominate at small momenta. Each massive

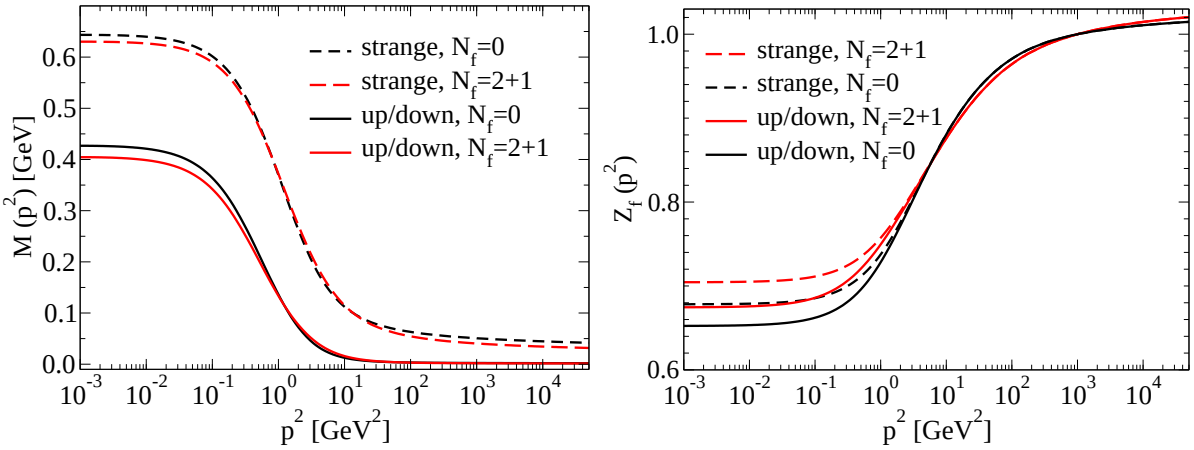

Figure 14. Unquenched quark propagator compared to quenched results. From: Fischer, Watson and Cassing [106].

propagator therefore decreases the degree of infrared singularity of the quark loop by a factor of p^2 compared to ghost and gluon loops. It is hard to see how the quark-gluon vertex should compensate for this. Therefore quark loops are almost certainly subleading in the infrared in their respective DSEs and cannot influence the infrared behaviour of Yang-Mills theory‖.

In the quark DSE unquenching effects are mediated only indirectly via the quark-gluon interaction, *i.e.* via the gluon propagator and the quark-gluon vertex. The resulting effects are much less pronounced than in the Yang-Mills sector, see figure 14. The quark mass function in the infrared is reduced by roughly 10% compared to the quenched case. This reduction has been seen for a range of truncations for the quark-gluon vertex [115] and is also confirmed by a lattice study employing staggered quarks [129]. The chiral condensate from unquenched DSE-solutions is hardly dependent on the number of flavours as long as $N_f \leq 3$ [106, 115]. Since the condensate is an order parameter for dynamical chiral symmetry breaking it is expected to change rapidly at the vicinity of the chiral phase transition. One may therefore conclude that the critical number of flavours for the chiral transition at zero temperature is much larger than $N_f = 3$. This agrees with our discussion at the beginning of this subsection.

3.3. Quarks in a box

Lattice simulations are, of course, always performed at a finite volume. This per se causes troubles in implementing chiral symmetry. In the introduction to this section I mentioned the need for lattice actions to satisfy the Ginsparg-Wilson relation. This ensures that a lattice variant of chiral symmetry is satisfied. However, even if this relation is satisfied there is more trouble ahead: chiral symmetry is continuous and can therefore not be spontaneously broken at any finite volume V. This means that a small 'seed' quark mass always has to be present on the lattice. Chiral symmetry is restored

‖ Certainly this need not be true for the chirally symmetric phase of QCD.

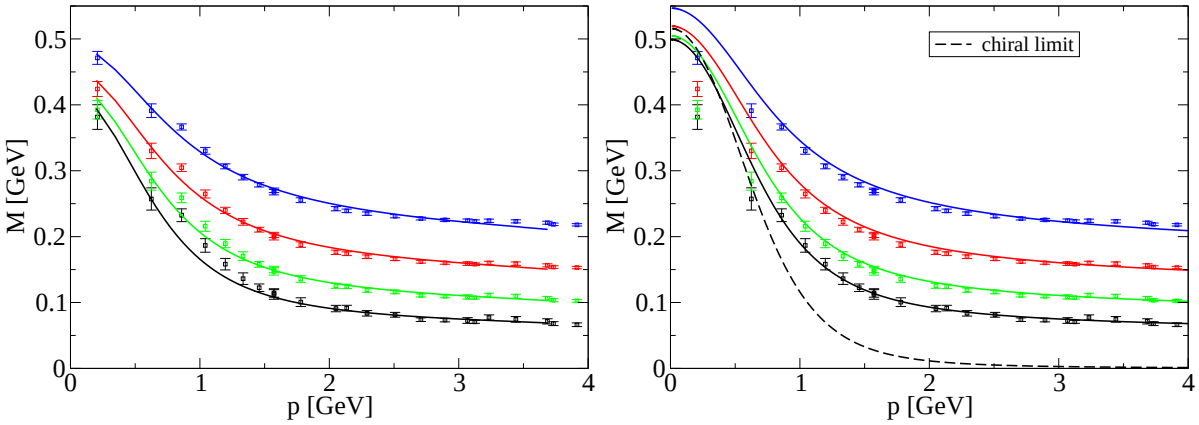

Figure 15. Results for the quark mass function M from Dyson-Schwinger equations compared with lattice data for overlap quarks. The DSE-solutions on the left diagram are obtained on a similar manifold as the lattice data, whereas in the right diagram infinite volume/continuum solutions are shown. From: Fischer and Pennington, [110] (DSE), Zhang *et al.* [135] (lattice).

in the limit of zero quark mass, $m \to 0$, independently of the formulation of the lattice action. Thus one has to perform the limit $V \to \infty$ first, before one can investigate the chiral limit [131]. In turn this means that lattice studies employing small quark masses are only meaningful if the volume of the underlying manifold is large enough. This is one of the reasons why it is extremely expensive in terms of CPU-time to simulate small quark masses. Volume effects are therefore a very important issue in the investigation of chiral symmetry breaking on compact manifolds.

Chiral perturbation theory on finite volumes is a reliable tool for the extrapolation of lattice results for meson and baryon observables (see e.g. [132–134] and references therein). However, chiral perturbation theory has nothing to say about volume effects in the underlying quark and gluon substructure. Furthermore, chiral perturbation theory builds upon the chiral limit, *i.e.* it can only be applied on volumes large enough such that small quark masses remain accessible. To this end the discrete momentum space induced by the boundary conditions of the box has to look almost like a continuum one. Correspondingly the box has to be large enough to allow for sufficiently small nonzero momenta. On a compact manifold the bosonic degrees of freedom have momenta $\mathbf{p} = 2\pi\mathbf{n}/L$ with $\mathbf{n}$ a vector of integers. Small nonzero momenta below a typical chiral symmetry breaking scale of $4\pi f_\pi$ are therefore only present if the condition

$$L >> \frac{1}{2f_\pi} \sim 1 \text{ fm} \tag{3.14}$$

is satisfied. Here f_π is the decay constant of the pion. *A priori* there is no way to say by how much L has to exceed 1 fm [134]. We will see shortly that this scale can be well estimated using the quark DSE on a torus.

In the Dyson-Schwinger approach volume effects can be studied continuously from very small to very large volumes by solving the DSEs on a compact manifold. Furthermore one has direct access to the infinite volume/continuum limit without

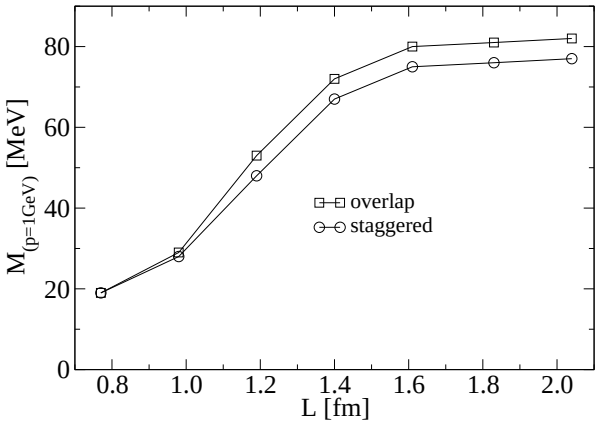

Figure 16. The quark mass function at a given momentum $p = 1$GeV plotted as a function of the box length L. From: Fischer and Pennington, [110].

extrapolations by solving the very same equations on R^4. One is thus in a position to study chiral symmetry restoration at small volumes together with effects at large and infinite volumes in one common framework. This idea is quite new and so far volume effects for the ghost and gluon propagator [100, 114] (*cf.* subsection 2.4) and the quark propagator [110] have been investigated. In the following I shortly summarize the results of the latter study.

As mentioned earlier, the quark-gluon vertex is the key element in the quark DSE. Following an idea of Bhagwat *et al.* [136] we modelled a simple approximation to this vertex such that quenched lattice data for various quark masses are reproduced on their manifold, *i.e.* by solutions to the quark DSE on a torus with the same volume as the lattice calculations. The results for the quark mass function is shown in the left diagram of figure 15, whereas the corresponding infinite volume/continuum results are shown in the right diagram of figure 15. The DSE-solutions on the torus reproduce the lattice data nicely. For small momenta, the DSE-results in the infinite volume/continuum limit differ sizeable from the results on the compact manifold. It is interesting to see that only the first two lattice points for each of the quark masses are affected by the finite volume. All other points follow the continuum solution. Similar effects have been found for a comparison with staggered quarks on the lattice. As a result we note that current lattice simulations may underestimate the amount of dynamical quark mass generation in the infrared by as much as 100 MeV.

A second interesting application of DSEs on a compact manifold concerns the abovementioned estimate of a minimal box length for chiral perturbation theory. To this end we employed a current quark mass of the order of a typical up/down-quark mass and determined the mass function $M(p^2)$ at $p^2 = 1$ GeV from solutions on tori with different volumes. The result is shown in figure 16. One observes that the quark mass function grows rapidly in the range $1.0 < L < 1.6$ fm signalling the onset of dynamical chiral symmetry breaking. Above $L = 1.6$ fm, a plateau is reached. This picture does not change when the mass function is extracted at smaller momenta or

when even smaller quark masses are employed. Thus a safe value for the minimal box length L should be at least

$$L_{\chi PT} \simeq 1.6 \text{ fm}. \tag{3.15}$$

This provides some justification for extending chiral perturbation theory to rather small volumes.

3.4. The analytical structure of the quark propagator

We have seen in subsection 2.5 that the transverse gluon cannot be part of the physical asymptotic state space of QCD, because its spectral function contains negative norm contributions. It is certainly interesting to investigate whether the same is true for the quark propagator. If the answer is yes, this constitutes an independent sign for quark confinement, no matter whether a linear rising potential for static quarks can be identified in Landau gauge or not (*c.f.* the discussion in subsection 2.1). The spectral properties of the quark propagator have been studied in a number of publications (see *e.g.* [4, 137–140] and references therein). Here I will concentrate on the most recent results, taken from [110, 116, 136, 141].

The method to determine the analytic structure of the quark propagator is the same as for the gluon propagator: one calculates the propagator for positive Euclidean momenta and determines the corresponding Schwinger function (2.19). One can then fit appropriate forms to the Schwinger function which reflect different analytical structures. A suitable form for the time dependence of the Schwinger function $\sigma(t)$ of (2.19) is (see [116] for details)

$$\sigma(t) = b_0 \exp(-b_1 t) \cos(b_2 t + b_3) \quad , \tag{3.16}$$

It can be shown that the exponential decay parameter b_1 corresponds to the real part of the leading singularity in the quark propagator. The parameter b_2 measures whether there is an imaginary part. If $b_2 = 0$ we have a positive definite quark with one pole on the real momentum axis, whereas $b_2 \neq 0$ corresponds to a pair of complex conjugate poles in the timelike momentum plane. This second form leads to negative norm contributions and therefore describes a confined quark.

Unfortunately it turns out that the quark is a much more difficult case than the gluon. The reason is to be found in the structure of the quark-gluon vertex. It has been demonstrated in [110, 116] that a sufficiently strong presence of a scalar part of the vertex has a significant impact on the analytical structure of the quark propagator. This is demonstrated in figure 17. Shown are results for the logarithm of the Schwinger function $\sigma(t)$, (i) employing a quark gluon vertex with a γ_μ-part only and (ii) substituting a construction of the form (3.12), which contains a strong scalar interaction as well. The oscillations seen for case (i) correspond to a quark propagator with complex conjugate poles. These are located at a 'quark mass' of $m = 516(20) \pm i\,428(20)$ MeV. The spikes in the curve indicate sign changes in the Schwinger function signalling negative norm contributions and therefore quark confinement. On the other hand,

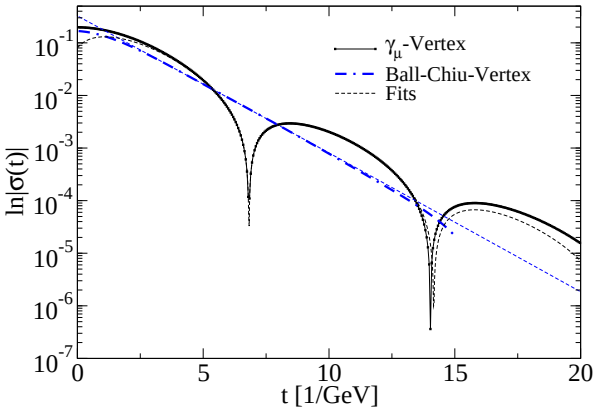

Figure 17. The logarithm of the Schwinger function $\ln(|\sigma(t)|)$ of the chiral limit quark propagator as a function of time. Shown are results, (i) employing a quark gluon vertex with a γ_μ-part only and (ii) substituting a construction of the form (3.12), which contains a strong scalar interaction. The results are compared to fits of the function (3.16). From: Fischer and Pennington, [110].

the exponentially decaying Schwinger function for case (ii) corresponds to a positive definite quark propagator with a pole on the real axis at $m = 632(20) \pm i\,0(2)$ MeV (within numerical accuracy). Although such a quark may still be confined via the BRST-quartet mechanism [40], this cannot be seen from the analytical structure of the quark propagator.

These results show that the analytic structure of the quark propagator depends strongly on the details of the structure of the quark-gluon vertex. A crucial point seems to be whether the scalar parts in the dressed quark-gluon vertex are of similar strength as in the ansatz (3.12) or not. Lattice data for the quark propagator alone cannot decide this question, since these can be reproduced by both a vertex with or without a strong scalar contribution [110]. It seems as if the only way to solve this problem is to analyse the quark-gluon vertex directly either on the lattice or by solving its DSE. First attempts in this direction on the lattice [120] as well as in the DSE approach [121–123] have been made, but have not yet reached a stage which allows definite statements. The analytical structure of the quark propagator therefore remains yet an open problem.

4. Light Mesons as bound states of quarks and gluons

In the last two sections I summarized the results of recent efforts to determine some fundamental properties of the elementary particles of QCD, the quarks and gluons. We have seen that their nonperturbative two-point functions are significantly different from their counterparts in perturbation theory. Certainly this comes as no surprise. Strong quantum fluctuations are to be expected to affect the properties of quarks and gluons since these are confined. In this section we will consider the impact of these results on observable properties of light mesons. The framework emerging from these efforts directly connects structures from the Yang-Mills- and the quark-sector of QCD with the

experiment.

I will first focus on probably the most important aspect of QCD when it comes to light mesons: the emergence of pseudoscalar mesons as the Goldstone bosons of dynamically broken chiral symmetry. I will then summarize recent efforts to explicitly include the gluonic substructure into the description of these mesons. This allows for a first investigation of unquenching effects in the pion and the rho meson. Finally I will summarize a broad range of results on experimental observables that have been obtained in the last years employing a simple model for the quark-gluon interaction. This last subsection is intended only as a short guide to the wealth of existing literature on this subject.

4.1. Goldstone bosons and quark-antiquark states

The pion as a bound state of a quark and an antiquark is described by the homogeneous Bethe-Salpeter equation (BSE) which can be written schematically as

$$\Gamma^\pi(p;P) \;=\; \int \frac{d^4k}{(2\pi)^4}\, K(p,k;P)\, S(k_+)\, \Gamma^\pi(k;P)\, S(k_-). \tag{4.1}$$

Here $\Gamma^\pi(p;P)$ is the Bethe-Salpeter amplitude of the pion and $K(p,k;P)$ is the so called Bethe-Salpeter kernel, which describes the interaction of the quark and the antiquark, with relative momentum p, inside a pion of momentum P. The momentum arguments $k_+ = k + \xi P$ and $k_- = k + (\xi - 1)P$ of the two quark propagators are defined such that the total momentum of the pion is given by $P = k_+ - k_-$. All physical results are independent of the momentum partitioning $\xi = [0,1]$ between the quark and the antiquark. Equation (4.1) can be easily adapted to describe mesons of arbitrary flavour content. The Bethe-Salpeter amplitude of any pseudoscalar particle including the pion can be decomposed into four Dirac-structures,

$$\Gamma^{PS}(p;P) \;=\; \gamma_5 \left(\Gamma_0(p;P) - \imath \not{P}\, \Gamma_1(p;P) - \imath \not{p}\, \Gamma_2(p;P) - [\not{P}, \not{p}]\, \Gamma_3(p;P)\right), \tag{4.2}$$

which can be determined separately from the BSE (4.1) once the interaction kernel K has been specified.

The crucial link between the meson bound states and their quark and gluon constituents is provided by the axial vector Ward-Takahashi identity (axWTI). Denoting the quark DSE (*cf.* figure 10) by

$$S^{-1}(p) = S_0^{-1}(p) - \Sigma(p) \tag{4.3}$$

one can write the axial vector Ward-Takahashi identity as

$$-\left[\Sigma(p_+)\gamma_5 + \gamma_5 \Sigma(p_-)\right] = \int \frac{d^4k}{(2\pi)^4} K(p,k;P)\left[\gamma_5 S(k_-) + S(k_+)\gamma_5\right], \tag{4.4}$$

where again all flavour and spinor indices have been omitted. We see that this identity demands a tight relation between the quark self-energy Σ and the Bethe-Salpeter kernel K. Maris, Roberts and Tandy have shown analytically that this relation ensures that the pion is a massless Goldstone boson in the chiral limit [142, 143]. Subsequently Bicudo

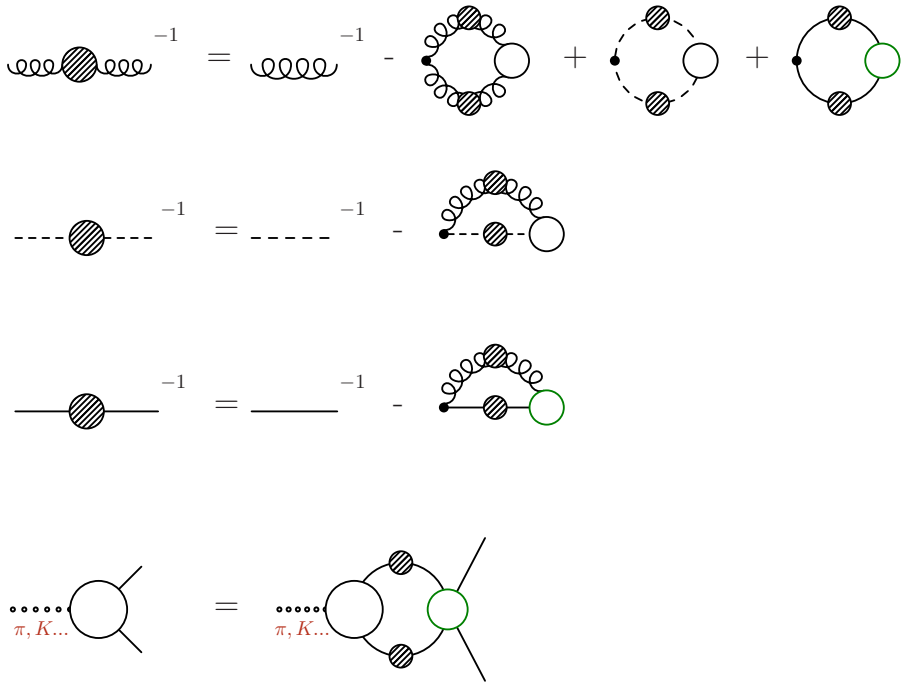

Figure 18. A diagrammatical representation of the coupled system of ghost, gluon and quark Schwinger-Dyson equations and the meson Bethe-Salpeter equation. Filled circles denote dressed propagators and empty circles denote dressed vertex functions.

et al [144] and Bicudo [145] established an analytic proof that Weinberg's low energy theorems for $\pi - \pi$ scattering, the Goldberger Treiman relation and the Adler zero in the chiral limit hold in all approximation schemes for the quark DSE and the Bethe-Salpeter kernel K that satisfy the axWTI. This establishes a profound understanding of the chiral properties of the pion in terms of the underlying gauge theory.

One example of a truncation scheme satisfying the axWTI is the well studied rainbow-ladder truncation (for reviews see [7, 11]). This truncation employs a specific form of the quark gluon vertex, which leads to rainbow-like diagrams in the quark DSE together with ladder-like diagrams in the Bethe-Salpeter equation. The Goldstone-boson nature of the pion is also manifest in the numerical solutions to such truncation schemes, as we will see in the next subsection.

4.2. Unquenching light mesons

As an example of an application of the DSE/BSE formalism I discuss recent attempts to implement and quantify unquenching effects in the description of light mesons. Depending on the observable under investigation these effects are qualitatively and quantitatively important. Unquenching is mandatory to describe meson decays like $\rho \to \pi\pi$. They are also anticipated to be important for scalar mesons where one deals with genuine quark-antiquark states or (admixtures of) meson-meson or even

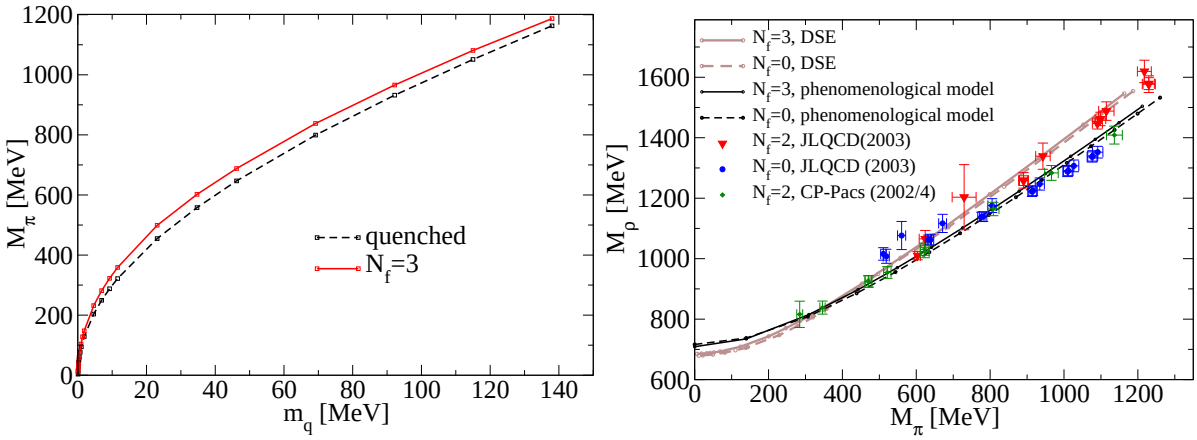

Figure 19. Left diagram: pseudoscalar meson masses as functions of the current quark mass for the quenched and unquenched theory with three degenerate sea quarks. Right diagram: Quenched and unquenched results for the vector meson mass as a function of the pseudoscalar meson mass. From: Fischer, Watson and Cassing [106] (DSE/BSE), CP-PACS collaboration [148, 149] and JLQCD collaboration [150] (lattice).

diquark-diquark correlations [146, 147]. The latter contributions are only present in the unquenched theory.

A systematic examination of unquenching effects in the quark-quark four-point function (related to the Bethe-Salpeter kernel K of equation (4.1)) has been carried out by Watson and Cassing [146]. They demonstrated that the unquenched four-point function contains physical resonances only, whereas unphysical diquark states are absent. Subsequently a quantitative analysis of a particular class of unquenching effects (quark loops in the gluon polarisation) has been carried out in [106]. To this end the coupled system of DSEs and BSEs shown diagrammatically in figure 18 has been solved. The employed quark-gluon vertex is a simplified version of (3.12). This vertex and the corresponding Bethe-Salpeter kernel are chosen such that the axWTI (4.4) is satisfied. The resulting pion is a massless Goldstone boson in the chiral limit as can be seen in the left diagram of figure 19. Plotted is the pion mass as a function of the current quark

Table 1. Parameter sets and results for the masses m_π, m_K, m_ρ and decay constants f_π, f_K for the quenched case ($N_f = 0$), the unquenched case with three degenerate 'sea'-quarks ($N_f = 3$) and the physical quark configuration case ($N_f = 2 + 1$) with two up/down quarks and one strange quark. The values for the current quark masses are evolved to $\mu = 2\,\mathrm{GeV}$ according to their one-loop behaviour. All units are given in MeV. From: Fischer, Watson and Cassing [106].

	m_u	m_s	m_π	f_π	m_K	f_K	m_ρ
$N_f = 0$	4.17	88.2	139.7	130.9	494.5	165.6	708.0
$N_f = 3$	4.06		139.7	130.8			690.0
$N_f = 2 + 1$	4.06	86.0	140.0	131.1	493.3	169.5	695.2
PDG[151]			139.6	130.7	493.7	160.0	770.0

mass at a fixed large renormalisation point. In the chiral limit, *i.e.* for $m_q \to 0$, one obtains $M_\pi \to 0$ without any finetuning.

A suitable quantity to compare the results with lattice data is the mass of the ρ-meson as a function of the pion mass. No scheme ambiguities arise since both quantities are physical. The results are shown in figure 19. Compared are results from the full DSE-setup, described above, with those obtained employing a phenomenological model for the quark-gluon interaction (the details of the model are described in [106]). The model interaction and the quark-gluon interaction of the complete set of DSEs are complementary to each other in the sense that the model interaction is confined to a quite narrow momentum region, whereas the interaction of the full DSE-setup has considerable strength in the infrared and extends into the ultraviolet according to the perturbative one-loop scaling. Together, both setups represent a measure for the theoretical error of the calculation. This error is of the same size as the combined systematic error of the different lattice simulations. In general, the results are in nice agreement with the lattice data. Below 240 MeV lattice data are not yet available. The results from the DSEs show a nonlinear dependence of the vector meson mass on the pseudoscalar one. The effect of unquenching – when viewed as a function of the pseudoscalar meson mass – becomes the same for both schemes: the vector meson mass is slightly increased when quark loops are taken into account. This trend is also seen in the lattice simulations, where the effect is even more pronounced. However, these unquenching effects are small compared to the differences between both the two truncation schemes that have been employed and the systematic errors of the lattice results.

The comparison of the results from the DSE/BSE approach with the lattice is encouraging, though there is still a lot of work to be done. The current truncation scheme for the DSE/BSEs has to be extended systematically to include the full tensor structure of the quark-gluon interaction. Furthermore the unquenched quark four-point function of [146] has to be incorporated to allow for effects due to the decay of the ρ-meson. Together, both improvements can be expected to bring the ρ-mass to its experimental value at the physical point in figure 19. The resulting $\rho - \pi$-mass curve should then agree with the one from chiral perturbation theory at small pion masses and with (potentially improved) lattice data at large pion-masses. If so, one has a framework which allows to extract and understand the internal structure of light mesons in terms of (nonperturbative) quarks and gluons.

4.3. Meson properties from BSEs

The framework described in the last subsection explicitly resolves the details of quark and gluon propagation and their interaction inside mesons. Such an approach is feasible at the expense of considerable technical and numerical effort. A technically simpler approach is to approximate the combination of the gluon propagator and the quark-gluon vertex by a model function. This approach provides interactions which are within the class of rainbow/ladder approximations that satisfy the axWTI. Thus the correct

behaviour of the pion as a Goldstone boson is guaranteed. These models have been explored extensively in the past years, leading to a range of interesting results. Some of these have been discussed in detail in recent reviews [7, 11]. I will only give a very brief overview here, which is intended as a short (and by far not exhaustive) guide to the literature.

The employed models for the combined gluon propagator and quark-gluon vertex are built upon the known perturbative ultraviolet limit and possess a certain interaction strength in the infrared which is controlled by a number of parameters (typically two or three). The central premise of such an account is the idea that the detailed shape of the interaction in the infrared is not important in the quark DSE. The integrated strength of this effective interaction between the quarks has to be sufficiently strong to induce spontaneous chiral symmetry breaking and associated dynamical quark mass generation. This idea has well known limitations in the scalar and axialvector meson sector [152–154] but turned out to be successful for the description of pseudoscalar and vector mesons.

Explicit calculations within such an approximation scheme explained the twofold nature of the pion as Goldstone boson and bound state of heavy constituents [142, 143]. The simultaneous absence of diquark states from the physical spectrum of (Landau gauge) QCD has been demonstrated in [152]†. Masses and decay constants of vector mesons have been determined in [156]. Corresponding results for strange and charmed pseudoscalar and vector mesons are reported in [157]. Detailed studies of the electromagnetic properties of ground state pseudoscalar mesons (charge radii, form factors, etc.) can be found in [158–160]. Results for radially excited pseudoscalar mesons have been reported recently in [161].

In addition to static properties of mesons also scattering processes have been analysed. Aspects of $\pi - \pi$ scattering have been investigated in [144, 145, 162] (*cf.* subsection 4.1). In particular the existence of the σ and ρ-resonances at the proper energies in $\pi - \pi$ scattering has been shown in [162]. In references [158, 163] it has been demonstrated that the cross section of the anomalous decay $\pi \to \gamma\gamma$ known from the perturbative triangle diagram is reproduced in rainbow/ladder approximation. Processes including the $\gamma{-}3\pi$ form factor are investigated in [164–167]. The results agree well with corresponding low energy theorems. Explicit decays like $\rho \to \pi\pi$, $\phi \to KK$ and $K^* \to \pi K$ are investigated in [168]. Aspects of the $U_A(1)$-problem and $\eta{-}\eta'$-mixing are analyzed in [169–171]. Conceptual issues and results for pion quark distributions have been discussed in [172, 173].

5. Concluding remarks

In this review I summarized recent results obtained from the framework of Dyson-Schwinger and Bethe-Salpeter equations in Landau gauge QCD. One of the issues I

† The corresponding absence of bound diquark states in Coulomb gauge has been reported recently in [155].

emphasized is the capability of this method to build bridges between different areas of quantum field theory. The approach connects the perturbative ultraviolet momentum regime with the nonperturbative low energy limit of the theory. It also connects hadron phenomenology with an underlying description of hadrons in terms of dressed quarks and gluons. The approach is complementary in its strengths and weaknesses to lattice gauge theory and therefore provides an alternative tool to analyse the theoretical structures of QCD.

The results in the Yang-Mills sector of QCD support a possible infrared effective theory which is given by the gauge-fixing parts of the action only. Ghost degrees of freedom dominate in the infrared and provide for long range correlations whereas the gluon propagator vanishes at zero momentum. We have seen that the latter property implies positivity violations in the gluon propagator. Transverse gluons are therefore confined. We analysed the behaviour of the running coupling of SU(N)-Yang-Mills theory in the infrared and found a fixed point which is (qualitatively) universal and invariant at least in a class of transverse gauges.

In the quark sector we discussed the effects of dynamical chiral symmetry breaking in the dressed quark propagator. Most of the mass of light quarks is generated dynamically. The chiral condensate can be extracted reliably from the quark propagator. Chiral symmetry breaking on a compact manifold has been studied. Probably the most notable result here is a minimal box length for chiral perturbation theory. In the meson sector of QCD we saw that the approach naturally reproduces the Goldstone nature of the pion as well as resulting low energy theorems. The applicability of the framework as a tool for hadron phenomenology is well explored. First steps have been made to explicitly investigate effects from the gauge sector of QCD in meson observables.

There are also a number of open problems that pose challenges for the future. The gluon self-interaction may be a key ingredient in our understanding of the transition from the perturbative to the nonperturbative region of Yang-Mills theory and needs to be further investigated. The detailed structure of the quark-gluon interaction and its consequences for the analytical structure of the quark propagator is not yet clarified. When it comes to comparison with lattice results an important open problem is the difference between the continuum results for the ghost and gluon propagators and the results on the compact manifold. Here one likes to see how exactly the continuum limit is approached when the volume of the compact manifold is increased. In general, it also seems promising to further explore the relation of the results in Landau gauge to other gauges as for example Coulomb gauge or the maximal Abelian gauge. Finally, unquenching the meson sector is a central issue in order to establish even closer contact with experiment.

Acknowledgments

It is a pleasure to thank Alan Martin for the invitation to write this review. I am grateful to Reinhard Alkofer, Wolfgang Cassing, Will Detmold, Holger Gies, Felipe

Llanes-Estrada, Pieter Maris, Mike Pennington, Hugo Reinhardt, Lorenz von Smekal, Peter Watson and Dan Zwanziger for pleasant and fruitful collaborations on some of the topics discussed here. Furthermore I would like to thank Mandar Bhagwat, Jacques Bloch, John Gracey, Andreas Krassnigg, Derek Leinweber, Orlando Oliveira, Jan Pawlowski, Craig Roberts, Paulo Silva, Jonivar Skullerud, Peter Tandy and Tony Williams for inspiring discussions and Reinhard Alkofer and Dominik Stoeckinger for a critical reading of the manuscript. This work has been supported by the GSI, Darmstadt and the Deutsche Forschungsgemeinschaft (DFG) under contract Fi 970/7-1.

References

[1] J. Greensite *Prog. Part. Nucl. Phys.* **51** (2003) 1, hep-lat/0301023.
[2] S. Chandrasekharan and U. J. Wiese *Prog. Part. Nucl. Phys.* **53** (2004) 373–418, hep-lat/0405024.
[3] J. M. Pawlowski hep-th/0512261.
[4] C. D. Roberts and A. G. Williams *Prog. Part. Nucl. Phys.* **33** (1994) 477–575, hep-ph/9403224.
[5] R. Alkofer and L. von Smekal *Phys. Rept.* **353** (2001) 281, hep-ph/0007355.
[6] C. D. Roberts and S. M. Schmidt *Prog. Part. Nucl. Phys.* **45** (2000) S1–S103, nucl-th/0005064.
[7] P. Maris and C. D. Roberts *Int. J. Mod. Phys.* **E12** (2003) 297–365, nucl-th/0301049.
[8] A. Maas *Mod. Phys. Lett.* **A20** (2005) 1797–1811, hep-ph/0506066.
[9] A. Maas, J. Wambach, and R. Alkofer *Eur. Phys. J.* **C42** (2005) 93–107, hep-ph/0504019.
[10] D. Nickel, J. Wambach, and R. Alkofer hep-ph/0603163.
[11] P. Maris and P. C. Tandy nucl-th/0511017.
[12] J. C. R. Bloch, C. D. Roberts, and S. M. Schmidt *Phys. Rev.* **C61** (2000) 065207, nucl-th/9911068.
[13] S. Ahlig *et al. Phys. Rev.* **D64** (2001) 014004, hep-ph/0012282.
[14] M. Oettel, R. Alkofer, and L. von Smekal *Eur. Phys. J.* **A8** (2000) 553–566, nucl-th/0006082.
[15] M. B. Hecht *et al. Phys. Rev.* **C65** (2002) 055204, nucl-th/0201084.
[16] R. Alkofer, A. Holl, M. Kloker, A. Krassnigg, and C. D. Roberts *Few Body Syst.* **37** (2005) 1–31, nucl-th/0412046.
[17] Y. L. Dokshitzer and D. E. Kharzeev *Ann. Rev. Nucl. Part. Sci.* **54** (2004) 487–524, hep-ph/0404216.
[18] L. von Smekal, R. Alkofer, and A. Hauck *Phys. Rev. Lett.* **79** (1997) 3591–3594, hep-ph/9705242.
[19] D. Atkinson and J. C. R. Bloch *Phys. Rev.* **D58** (1998) 094036, hep-ph/9712459.
[20] P. Watson and R. Alkofer *Phys. Rev. Lett.* **86** (2001) 5239, hep-ph/0102332.
[21] D. Zwanziger *Phys. Rev.* **D65** (2002) 094039, hep-th/0109224.
[22] C. Lerche and L. von Smekal *Phys. Rev.* **D65** (2002) 125006, hep-ph/0202194.
[23] D. Zwanziger *Phys. Rev.* **D67** (2003) 105001, hep-th/0206053.
[24] F. D. R. Bonnet, P. O. Bowman, D. B. Leinweber, and A. G. Williams *Phys. Rev.* **D62** (2000) 051501, hep-lat/0002020.
[25] F. D. R. Bonnet, P. O. Bowman, D. B. Leinweber, A. G. Williams, and J. M. Zanotti *Phys. Rev.* **D64** (2001) 034501, hep-lat/0101013.
[26] K. Langfeld, H. Reinhardt, and J. Gattnar *Nucl. Phys.* **B621** (2002) 131–156, hep-ph/0107141.
[27] A. Cucchieri and D. Zwanziger *Phys. Lett.* **B524** (2002) 123–128, hep-lat/0012024.
[28] F. Halzen and A. D. Martin, "Quarks and Leptons: an introductory course in modern particle physics,". New York, Usa: Wiley (1984) 396p.

[29] M. E. Peskin and D. V. Schroeder, "An Introduction to quantum field theory,". Reading, USA: Addison-Wesley (1995) 842 p.
[30] R. J. Rivers, "Path Integral Methods In Quantum Field Theory,". Cambridge, UK: Univ. Pr. (1987) 339 p. (Cambridge monographs on mathematical physics).
[31] L. D. Faddeev and V. N. Popov *Phys. Lett.* **B25** (1967) 29–30.
[32] S. Pokorski, "Gauge Field Theories,". Cambridge, Uk: Univ. Pr. (1987) 394 P. (Cambridge Monographs On Mathematical Physics).
[33] A. G. Williams *Nucl. Phys. Proc. Suppl.* **109A** (2002) 141–145, hep-lat/0202010.
[34] C. Becchi, A. Rouet, and R. Stora *Annals Phys.* **98** (1976) 287–321.
[35] M. Z. Iofa and I. V. Tyutin *Teor. Mat. Fiz.* **27** (1976) 38–47.
[36] K. Fujikawa *Nucl. Phys.* **B223** (1983) 218.
[37] L. Baulieu and M. Schaden *Int. J. Mod. Phys.* **A13** (1998) 985–1012, hep-th/9601039.
[38] T. Kugo, "Eichtheorie,". Berlin, Germany: Springer Verlag (1997) 522 P. (in German only).
[39] T. Kugo and I. Ojima *Prog. Theor. Phys. Suppl.* **66** (1979) 1.
[40] N. Nakanishi and I. Ojima, "Covariant operator formalism of gauge theories and quantum gravity," *World Sci. Lect. Notes Phys.* **27** (1990) 1–434.
[41] C. S. Fischer hep-ph/0304233.
[42] T. Kugo hep-th/9511033.
[43] K. Osterwalder and R. Schrader *Commun. Math. Phys.* **31** (1973) 83–112.
[44] K. Osterwalder and R. Schrader *Commun. Math. Phys.* **42** (1975) 281.
[45] V. N. Gribov *Nucl. Phys.* **B139** (1978) 1.
[46] D. Zwanziger *Phys. Rev.* **D69** (2004) 016002, hep-ph/0303028.
[47] A. Cucchieri *Nucl. Phys.* **B508** (1997) 353–370, hep-lat/9705005.
[48] J. E. Mandula *Phys. Rept.* **315** (1999) 273–284, hep-lat/9907020.
[49] C. Alexandrou, P. de Forcrand, and E. Follana *Phys. Rev.* **D63** (2001) 094504, hep-lat/0008012.
[50] C. Alexandrou, P. de Forcrand, and E. Follana *Phys. Rev.* **D65** (2002) 114508, hep-lat/0112043.
[51] C. Alexandrou, P. De Forcrand, and E. Follana *Phys. Rev.* **D65** (2002) 117502, hep-lat/0203006.
[52] L. Giusti, M. L. Paciello, C. Parrinello, S. Petrarca, and B. Taglienti *Int. J. Mod. Phys.* **A16** (2001) 3487–3534, hep-lat/0104012.
[53] P. J. Silva and O. Oliveira *Nucl. Phys.* **B690** (2004) 177–198, hep-lat/0403026.
[54] S. Furui and H. Nakajima *Phys. Rev.* **D70** (2004) 094504.
[55] A. Sternbeck, E. M. Ilgenfritz, M. Mueller-Preussker, and A. Schiller *Phys. Rev.* **D72** (2005) 014507, hep-lat/0506007.
[56] A. Y. Lokhov, O. Pene, and C. Roiesnel hep-lat/0511049.
[57] I. L. Bogolubsky, G. Burgio, M. Muller-Preussker, and V. K. Mitrjushkin hep-lat/0511056.
[58] D. Zwanziger *Nucl. Phys.* **B518** (1998) 237–272.
[59] A. Cucchieri and D. Zwanziger *Phys. Rev.* **D65** (2002) 014002, hep-th/0008248.
[60] D. Zwanziger *Phys. Rev. Lett.* **90** (2003) 102001, hep-lat/0209105.
[61] A. P. Szczepaniak and E. S. Swanson *Phys. Rev.* **D65** (2002) 025012, hep-ph/0107078.
[62] J. Greensite and S. Olejnik *Phys. Rev.* **D67** (2003) 094503, hep-lat/0302018.
[63] D. Zwanziger *Phys. Rev.* **D70** (2004) 094034, hep-ph/0312254.
[64] C. Feuchter and H. Reinhardt *Phys. Rev.* **D70** (2004) 105021, hep-th/0408236.
[65] A. Nakamura and T. Saito hep-lat/0512042.
[66] C. S. Fischer and D. Zwanziger *Phys. Rev.* **D72** (2005) 054005, hep-ph/0504244.
[67] D. Zwanziger *Nucl. Phys.* **B399** (1993) 477–513.
[68] D. Zwanziger *Nucl. Phys.* **B364** (1991) 127–161.
[69] C. Itzykson and J. B. Zuber, "Quantum Field Theory,". New York, Usa: Mcgraw-hill (1980) 705 P.(International Series In Pure and Applied Physics).

[70] V. Sauli hep-ph/0412188.
[71] L. von Smekal, A. Hauck, and R. Alkofer *Ann. Phys.* **267** (1998) 1, hep-ph/9707327.
[72] D. Atkinson and J. C. R. Bloch *Mod. Phys. Lett.* **A13** (1998) 1055–1062, hep-ph/9802239.
[73] J. C. R. Bloch *Phys. Rev.* **D64** (2001) 116011, hep-ph/0106031.
[74] W. Schleifenbaum, A. Maas, J. Wambach, and R. Alkofer *Phys. Rev.* **D72** (2005) 014017, hep-ph/0411052.
[75] R. Alkofer, C. S. Fischer, and F. J. Llanes-Estrada *Phys. Lett.* **B611** (2005) 279–288, hep-th/0412330.
[76] J. C. Taylor *Nucl. Phys.* **B33** (1971) 436–444.
[77] A. Cucchieri, T. Mendes, and A. Mihara *JHEP* **12** (2004) 012, hep-lat/0408034.
[78] A. Sternbeck, E. M. Ilgenfritz, M. Muller-Preussker, and A. Schiller *PoS* **LAT2005** (2005) 333, hep-lat/0509090.
[79] J. M. Pawlowski, D. F. Litim, S. Nedelko, and L. von Smekal *Phys. Rev. Lett.* **93** (2004) 152002, hep-th/0312324.
[80] C. S. Fischer and H. Gies *JHEP* **10** (2004) 048, hep-ph/0408089.
[81] M. Baldicchi and G. M. Prosperi *Phys. Rev.* **D66** (2002) 074008, hep-ph/0202172.
[82] S. J. Brodsky, S. Menke, C. Merino, and J. Rathsman *Phys. Rev.* **D67** (2003) 055008, hep-ph/0212078.
[83] G. Grunberg hep-ph/0603135.
[84] A. C. Mattingly and P. M. Stevenson *Phys. Rev.* **D49** (1994) 437–450, hep-ph/9307266.
[85] D. V. Shirkov and I. L. Solovtsov *Phys. Rev. Lett.* **79** (1997) 1209–1212, hep-ph/9704333.
[86] D. V. Shirkov *Eur. Phys. J.* **C22** (2001) 331–340, hep-ph/0107282.
[87] D. M. Howe and C. J. Maxwell *Phys. Rev.* **D70** (2004) 014002, hep-ph/0303163.
[88] A. V. Nesterenko and J. Papavassiliou *Phys. Rev.* **D71** (2005) 016009, hep-ph/0410406.
[89] K. A. Milton, I. L. Solovtsov, and O. P. Solovtsova hep-ph/0512209.
[90] H. Gies *Phys. Rev.* **D66** (2002) 025006, hep-th/0202207.
[91] W. Celmaster and R. J. Gonsalves *Phys. Rev.* **D20** (1979) 1420.
[92] P. Pascual and R. Tarrach *Nucl. Phys.* **B174** (1980) 123.
[93] U. Ellwanger, M. Hirsch, and A. Weber *Z. Phys.* **C69** (1996) 687–698, hep-th/9506019.
[94] S. J. Brodsky *Fizika* **B13** (2004) 91–114, hep-ph/0310289.
[95] G. Grunberg *Phys. Rev.* **D29** (1984) 2315.
[96] A. Deur, V. Burkert, J. P. Chen, and W. Korsch hep-ph/0509113.
[97] W. Schleifenbaum, M. Leder, and H. Reinhardt hep-th/0605115.
[98] D. Dudal *et al. JHEP* **07** (2005) 059, hep-th/0505037.
[99] M. A. L. Capri *et al.* hep-th/0603167.
[100] C. S. Fischer, B. Gruter, and R. Alkofer *Annals of Physics in print* (2006) hep-ph/0506053.
[101] P. J. Silva and O. Oliveira hep-lat/0511043.
[102] P. Boucaud *et al.* hep-ph/0507104.
[103] A. Cucchieri and T. Mendes hep-lat/0602012.
[104] C. S. Fischer and R. Alkofer *Phys. Lett.* **B536** (2002) 177–184, hep-ph/0202202.
[105] J. C. R. Bloch *Few Body Syst.* **33** (2003) 111–152, hep-ph/0303125.
[106] C. S. Fischer, P. Watson, and W. Cassing *Phys. Rev.* **D72** (2005) 094025, hep-ph/0509213.
[107] B. Alles *et al. Nucl. Phys.* **B502** (1997) 325–342, hep-lat/9605033.
[108] P. Boucaud *et al. JHEP* **04** (2003) 005, hep-ph/0212192.
[109] P. O. Bowman, U. M. Heller, D. B. Leinweber, M. B. Parappilly, and A. G. Williams *Phys. Rev.* **D70** (2004) 034509, hep-lat/0402032.
[110] C. S. Fischer and M. R. Pennington *Phys. Rev.* **D73** (2006) 034029, hep-ph/0512233.
[111] A. C. Aguilar and A. A. Natale *JHEP* **08** (2004) 057, hep-ph/0408254.
[112] H. R. T. Tok, K. Langfeld and L. von Smekal hep-lat/0509134.
[113] P. Boucaud *et al.* hep-lat/0602006.
[114] C. S. Fischer, R. Alkofer, and H. Reinhardt *Phys. Rev.* **D65** (2002) 094008, hep-ph/0202195.

[115] C. S. Fischer and R. Alkofer *Phys. Rev.* **D67** (2003) 094020, hep-ph/0301094.
[116] R. Alkofer, W. Detmold, C. S. Fischer, and P. Maris *Phys. Rev.* **D70** (2004) 014014, hep-ph/0309077.
[117] V. A. Miransky *Phys. Lett.* **B165** (1985) 401–404.
[118] K. Langfeld, H. Markum, R. Pullirsch, C. D. Roberts, and S. M. Schmidt *Phys. Rev.* **C67** (2003) 065206, nucl-th/0301024.
[119] J. S. Ball and T.-W. Chiu *Phys. Rev.* **D22** (1980) 2542.
[120] J. I. Skullerud, P. O. Bowman, A. Kizilersu, D. B. Leinweber, and A. G. Williams *JHEP* **04** (2003) 047, hep-ph/0303176.
[121] M. S. Bhagwat and P. C. Tandy *Phys. Rev.* **D70** (2004) 094039, hep-ph/0407163.
[122] M. S. Bhagwat, A. Holl, A. Krassnigg, C. D. Roberts, and P. C. Tandy *Phys. Rev.* **C70** (2004) 035205, nucl-th/0403012.
[123] C. S. Fischer, F. Llanes-Estrada, and R. Alkofer *Nucl. Phys. Proc. Suppl.* **141** (2005) 128–133, hep-ph/0407294.
[124] W. J. Marciano and H. Pagels *Phys. Rept.* **36** (1978) 137.
[125] **ALPHA** Collaboration, S. Capitani, M. Luscher, R. Sommer, and H. Wittig *Nucl. Phys.* **B544** (1999) 669–698, hep-lat/9810063.
[126] V. Gimenez, V. Lubicz, F. Mescia, V. Porretti, and J. Reyes *Eur. Phys. J.* **C41** (2005) 535–544, hep-lat/0503001.
[127] J. Wennekers and H. Wittig *JHEP* **09** (2005) 059, hep-lat/0507026.
[128] H. Gies and J. Jaeckel *Eur. Phys. J.* **C46** (2006) 433–438, hep-ph/0507171.
[129] P. O. Bowman *et al. Phys. Rev.* **D71** (2005) 054507, hep-lat/0501019.
[130] S. Furui and H. Nakajima hep-lat/0511045.
[131] H. Leutwyler and A. Smilga *Phys. Rev.* **D46** (1992) 5607–5632.
[132] W. Detmold, W. Melnitchouk, J. W. Negele, D. B. Renner, and A. W. Thomas *Phys. Rev. Lett.* **87** (2001) 172001, hep-lat/0103006.
[133] M. Procura, T. R. Hemmert, and W. Weise *Phys. Rev.* **D69** (2004) 034505, hep-lat/0309020.
[134] G. Colangelo, S. Durr, and C. Haefeli *Nucl. Phys.* **B721** (2005) 136–174, hep-lat/0503014.
[135] J. B. Zhang *et al. Phys. Rev.* **D71** (2005) 014501, hep-lat/0410045.
[136] M. S. Bhagwat, M. A. Pichowsky, C. D. Roberts, and P. C. Tandy *Phys. Rev.* **C68** (2003) 015203, nucl-th/0304003.
[137] G. Krein, C. D. Roberts, and A. G. Williams *Int. J. Mod. Phys.* **A7** (1992) 5607–5624.
[138] C. J. Burden, C. D. Roberts, and A. G. Williams *Phys. Lett.* **B285** (1992) 347–353.
[139] P. Maris and H. A. Holties *Int. J. Mod. Phys.* **A7** (1992) 5369–5386.
[140] C. J. Burden *Phys. Rev.* **D57** (1998) 276–286, hep-ph/9702411.
[141] R. Alkofer, W. Detmold, C. S. Fischer, and P. Maris *Nucl. Phys. Proc. Suppl.* **141** (2005) 122–127, hep-ph/0309078.
[142] P. Maris, C. D. Roberts, and P. C. Tandy *Phys. Lett.* **B420** (1998) 267–273, nucl-th/9707003.
[143] P. Maris, C. D. Roberts, and P. C. Tandy *Phys. Lett.* **B420** (1998) 267–273, nucl-th/9707003.
[144] P. Bicudo *et al. Phys. Rev.* **D65** (2002) 076008, hep-ph/0112015.
[145] P. Bicudo *Phys. Rev.* **C67** (2003) 035201, hep-ph/0311277.
[146] P. Watson and W. Cassing *Few Body Syst.* **35** (2004) 99–115, hep-ph/0405287.
[147] M. R. Pennington hep-ph/0604212.
[148] **CP-PACS** Collaboration, A. Ali Khan *et al. Phys. Rev.* **D65** (2002) 054505, hep-lat/0105015.
[149] **CP-PACS** Collaboration, Y. Namekawa *et al. Phys. Rev.* **D70** (2004) 074503, hep-lat/0404014.
[150] **JLQCD** Collaboration, S. Aoki *et al. Phys. Rev.* **D68** (2003) 054502, hep-lat/0212039.
[151] **Particle Data Group** Collaboration, S. Eidelman *et al. Phys. Lett.* **B592** (2004) 1.
[152] A. Bender, C. D. Roberts, and L. Von Smekal *Phys. Lett.* **B380** (1996) 7–12, nucl-th/9602012.
[153] R. Alkofer, P. Watson, and H. Weigel *Phys. Rev.* **D65** (2002) 094026, hep-ph/0202053.
[154] P. Watson, W. Cassing, and P. C. Tandy *Few Body Syst.* **35** (2004) 129–153, hep-ph/0406340.

[155] R. Alkofer, M. Kloker, A. Krassnigg, and R. F. Wagenbrunn *Phys. Rev. Lett* **96** (2006) 022001, hep-ph/0510028.
[156] P. Maris and P. C. Tandy *Phys. Rev.* **C60** (1999) 055214, nucl-th/9905056.
[157] A. Krassnigg and P. Maris *J. Phys. Conf. Ser.* **9** (2005) 153–160, nucl-th/0412058.
[158] P. Maris and C. D. Roberts *Phys. Rev.* **C58** (1998) 3659–3665, nucl-th/9804062.
[159] P. Maris and P. C. Tandy *Phys. Rev.* **C61** (2000) 045202, nucl-th/9910033.
[160] P. Maris and P. C. Tandy *Phys. Rev.* **C62** (2000) 055204, nucl-th/0005015.
[161] A. Holl, A. Krassnigg, P. Maris, C. D. Roberts, and S. V. Wright *Phys. Rev.* **C71** (2005) 065204, nucl-th/0503043.
[162] S. R. Cotanch and P. Maris *Phys. Rev.* **D66** (2002) 116010, hep-ph/0210151.
[163] D. Kekez and D. Klabucar *Phys. Lett.* **B457** (1999) 359–367, hep-ph/9812495.
[164] R. Alkofer and C. D. Roberts *Phys. Lett.* **B369** (1996) 101–107, hep-ph/9510284.
[165] B. Bistrovic and D. Klabucar *Phys. Rev.* **D61** (2000) 033006, hep-ph/9907515.
[166] B. Bistrovic and D. Klabucar *Phys. Lett.* **B478** (2000) 127–136, hep-ph/9912452.
[167] S. R. Cotanch and P. Maris *Phys. Rev.* **D68** (2003) 036006, nucl-th/0308008.
[168] D. Jarecke, P. Maris, and P. C. Tandy *Phys. Rev.* **C67** (2003) 035202, nucl-th/0208019.
[169] L. von Smekal, A. Mecke, and R. Alkofer hep-ph/9707210.
[170] D. Klabucar and D. Kekez *Phys. Rev.* **D58** (1998) 096003, hep-ph/9710206.
[171] D. Kekez, D. Klabucar, and M. D. Scadron *J. Phys.* **G26** (2000) 1335–1354, hep-ph/0003234.
[172] M. B. Hecht, C. D. Roberts, and S. M. Schmidt *Phys. Rev.* **C63** (2001) 025213, nucl-th/0008049.
[173] B. C. Tiburzi, W. Detmold, and G. A. Miller *Phys. Rev.* **D68** (2003) 073002, hep-ph/0305190.